INTERNATIONAL ATOMIC ENERGY AGENCY
UNITED NATIONS EDUCATIONAL, SCIENTIFIC AND CULTURAL ORGANIZATION

INTERNATIONAL CENTRE FOR THEORETICAL PHYSICS
34100 TRIESTE (ITALY) - P.O.B. 586 - MIRAMARE - STRADA COSTIERA 11 - TELEPHONE: 2240-1
CABLE: CENTRATOM - TELEX 460392 - I

SMR/406-16

THIRD AUTUMN WORKSHOP ON ATMOSPHERIC
RADIATION AND CLOUD PHYSICS
27 November - 15 December 1989

"Radiative Transfer Equation in the Atmosphere: Its Application to the Remote Sensing Passive Measurements Performed by Airborne Platforms"

Rodolfo GUZZI
Istituto per lo Studio delle
Metololgie Geofisiche Ambientali
Modena
ITALY

Please note: These are preliminary notes intended for internal distribution only.

Radiative Transfer Equation in the Atmosphere:
Its Application to the Remote Sensing Passive Measurements Performed by Airborne Platforms

Rodolfo Guzzi

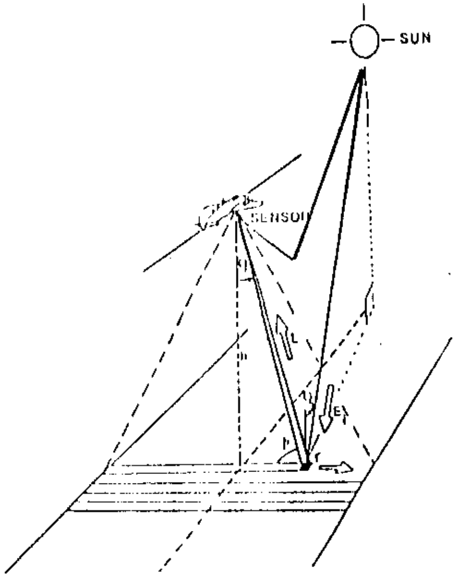

ISTITUTO PER LO STUDIO DELLE METODOLOGIE GEOFISICHE AMBIENTALI
(I M G A - C N R)
770 Emilia Est, 41100 Modena, Italy
Tel. (059) 362388

Technical Report No. 1–89

1 Introduction

In the last ten years solutions of the equation of radiative transfer in the atmosphere have been applied in different fields.

Remote sensing techniques, the use of renewable energies, studies of biological and chemical processes in the environment have benefitted from the knowledge of radiative mechanisms in the short and longwave ranges of the atmospheric spectrum.

In particular remote sensing applications on the environmental properties such as albedo and temperature of the surface together with the remote sounding of the atmosphere have been developed.

On the basis of the modification of the electromagnetic field due to the presence of gases and particulate matter in the atmosphere, it has been possible to describe the properties of the Earth's surface and atmosphere.

The interaction processes between radiation and matter require knowledge of the amplitude, the phase and the position of the oscillation plane of the waves interacting. The solutions of the radiative transfer equations contain these processes provided that proper boundary conditions are used. This paper deals with the solutions of the radiative transfer equation in view of applications in the field of remote sensing. In the second and third paragraphs the Radiative Transfer Equation and its solutions in atmosphere are shown. In the fourth paragraph the remote sensing applications are presented.

2 The Radiative Transfer Equation in Atmosphere

Let us consider an atmospheric volume; radiation travelling in the direction of a sensor is attenuated in the volume according to the extinction law.

Some photons are absorbed and some photons are scattered along the path of observation. Photons, created in the volume, are also emitted into the direction of observation.

So the Radiative Transfer Equation RTE can be written with an extinction term and an additional term taking into account intensification processes.

Then the amount of radiation lost and gained is:

$$dL(\lambda) = -\alpha(\lambda)L(\lambda)dz + \alpha(\lambda)J(\lambda)dz \tag{1}$$

where $\alpha(\lambda)$ is the absorption coefficient and L is the radiance. In differential form the RTE becomes:

$$\frac{dL(\lambda)}{\alpha(\lambda)dz} = -L(\lambda) + J(\lambda) \tag{2}$$

The $J(\lambda)$ function, or source function describing the intensification processes, is the sum of the following three terms:

1. the function $J_{diff}(\lambda)$ describing the diffusion mechanisms due to the diffuse radiation coming from surrounding volume
2. the function $J_{dir}(\lambda)$ describing the scattering mechanisms due to solar direct radiation
3. the function $J_e(\lambda)$ describing the emission mechanisms.

In order to locate the radiation field in atmosphere we introduce:

a. the optical depth, instead of the usual geometric altitude z, defined as:

$$\tau(\lambda) = \int_z^\infty \alpha(\lambda, z)dz = \int_z^\infty k(\lambda, z)\rho(z)dz \tag{3}$$

from the top of the atmosphere ∞ down to the height z. In addition we introduce also the atmospheric optical thickness

$$\tau_0(\lambda) = \int_0^\infty \alpha(\lambda, z)dz \tag{4}$$

where $k(\lambda, z)$ is the absorption coefficient (cm^2g^{-1}) and $\rho(z)$ is the density of the absorbing gases.

b. a spherical coordinate system in order to specify every point of the atmosphere itself. So each coordinate z, x, y is defined by the zenith angle θ and azimuthal angle φ. Frequently the quantity $\mu = \cos\theta$ is used. In fig. 1 the coordinates and the interaction between the light and the atmospheric volume are specified.

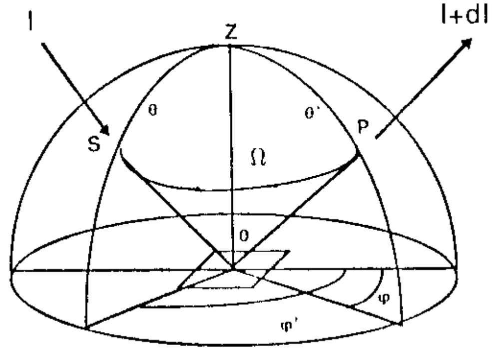

Fig. 1 Angle Ω is found by solving the spherical triangle S, Z, P formed by the three circle arcs defined by θ, θ' and the projection $(\varphi' - \varphi)$

c. As additional convention, upwelling radiation is identified by sign plus (+) and downwelling radiation by sign minus (−).

d. subscript zero (0) identifies solar radiation

e. the direction of the outgoing radiation is identified by primes (′)

f. the scattering angle Ω is connected to the above coordinates by

$$\cos\Omega = \mu \cdot \mu' + \sqrt{1-\mu'^2} \cdot \sqrt{1-\mu^2} \cdot \cos(\varphi - \varphi') \tag{5}$$

With these coordinates in mind we can write the source functions.

1. The source function of the photons describing the diffusion processes is:

$$J_{diff}(\lambda) = \frac{\omega_0(\lambda)}{4\pi} \int_0^{2\pi} \int_{-1}^{+1} L(\lambda, \tau, \mu, \varphi) P(\lambda, \mu', \varphi'; \mu, \varphi)\, d\mu\, d\varphi \tag{6}$$

2. The source function of the photons created by the illumination of direct solar radiation is:

$$J_{dir}(\lambda) = \frac{\omega_0(\lambda)}{4\pi} E_0(\lambda) \exp\left\{-\frac{\tau(\lambda)}{\mu_0}\right\} P(\lambda, \mu', \varphi'; -\mu_0, \varphi_0) \tag{7}$$

   where $E_0(\lambda)$ is the solar extraterrestrial irradiance.

3. The source function of the photons created in the atmospheric volume is:

$$J_e(\lambda, T^*) = [1 - \omega_0(\lambda)] B(\lambda, T^*) \tag{8}$$

   where $B(\lambda, T^*)$ is simply the Planck blackbody radiance at wavelenght λ and temperature T^*.

The albedo of single scattering, $\omega_0(\lambda)$, is the ratio of the amount of scattered flux to that scattered and absorbed i.e.:

$$\omega_0(\lambda) = \frac{\tau_{scat}(\lambda)}{\tau_{scat}(\lambda) + \tau_{abs}(\lambda)} \tag{9}$$

where τ_{scat} is the scattering optical depth and τ_{abs} is the absorption optical depth. The scattering phase function $P\big(\lambda, \Omega(\mu, \varphi; \mu'\varphi'; -\mu_o, \varphi_0)\big)$ is the ratio of scattered energy per unit solid angle in a given direction to the average energy scattered in all directions. This definition requires that the phase function be normalized to unity i.e.:

$$\frac{1}{4\pi} \int_0^{4\pi} P(\lambda, \Omega) d\omega = 1$$

where ω is the solid angle. With the present choice $d\omega = 2\pi \sin\Omega\, d\Omega$. Then we have:

$$\frac{1}{2} \int_0^{\pi} P(\lambda, \Omega) \sin\Omega\, d\Omega = 1 \tag{10}$$

Then the Radiative Transfer Equation (RTE) can be written:

$$\mu \frac{dL(\lambda, \tau, \Omega)}{d\tau(\lambda)} = -L(\lambda, \tau, \Omega) + J_{diff}(\lambda, \tau, \Omega) + J_{dir}(\lambda, \tau, \Omega) + J_e(\lambda, T^*) \tag{11}$$

3 Application of the Radiative Transfer Equation to different spectral intervals

3.1 Visible and near infrared spectrum

Since in the visible and near infrared the source function of the emission is negligible, RTE can be written with the convention adopted, as:

$$\mu \frac{dL(\lambda, \tau, (\lambda)\mu, \varphi)}{d\tau(\lambda)} = +L(\lambda, \tau(\lambda), \mu, \varphi) - \frac{\omega_0(\lambda)}{4\pi} E_0(\lambda) \cdot P(\lambda, \mu', \varphi'; -\mu_0, \varphi_0) \cdot \exp\left\{-\frac{\tau(\lambda)}{\mu_0}\right\} - \frac{\omega_0(\lambda)}{4\pi} \int_0^{2\pi} \int_{-1}^{+1} L(\lambda, \tau(\lambda), \mu, \varphi,) P(\lambda, \mu', \varphi', \mu, \varphi) d\,\mu\; d\,\varphi \tag{12}$$

In this equation the first term is the extinction of diffuse radiance crossing the incremental optical depth $d\,\tau(\lambda)$, with $\tau(\lambda) = 0$ at the top of the atmosphere and $\tau(\lambda) = \tau_0(\lambda)$ at the surface. The second term gives the rate of production of the radiance scattered out of the direct beam and the last term is the multiple scattering term.

Let us study now the three different cases from which we deduce the following models:

Case a. *Direct spectral solar irradiance model.*

Let us consider a plane-parallel atmosphere of optical thickness $\tau_0(\lambda)$ irradiated by the extraterrestrial solar irradiance $E_0(\lambda)$ (this is modified by standard orbital correction factor in order to take into account simulations at a specific time of year). The direct spectral irradiance $E_d(\lambda)$ on a horizontal plane at the surface of the Earth is given by:

$$\begin{aligned} E_d(\lambda) &= E_0(\lambda)\mu_0 \exp\left\{-\frac{\tau_0(\lambda)}{\mu_0}\right\} \\ &= E_0(\lambda)\mu_0 T(\tau(\lambda),\mu_0) \end{aligned} \tag{13}$$

where $T(\tau(\lambda),\mu_0)$ is the transmittance function which can be expressed as the product of transmittances due to scattering $T_{scat}(\tau(\lambda),\mu_0)$ and absorption processes $T_{abs}(\tau(\lambda),\mu_0)$

Thus, taking into account the atmospheric structure (see for instance Guzzi, (1988)) the transmittance function is due to the product of the transmittance functions expressing the molecular atmosphere, T_R, (Rayleigh scattering); ozone, T_{03}, water vapor, T_w; uniformly mixed gases, T_{mg}; (see Kneizys et al. 1983) and aerosol, T_a, (aerosol scattering). The equation (14) can be written as:

$$\begin{aligned} E(\lambda) &= E_0(\lambda)\mu_0 T_{scat}\big(\tau(\lambda),\mu_0\big) T_{abs}\big(\tau(\lambda),\mu_0\big) \\ E(\lambda) &= E_0(\lambda)\mu_0 T_w T_R T_{03} T_{mg} T_a \end{aligned} \tag{14}$$

where the dependence of transmittance functions on $\tau(\lambda)$ and μ_0, for compactness, has been omitted.

The amount of flux absorbed out of the direct beam is:

$$\begin{aligned} E_{abs}(\lambda) &= E_0(\lambda)\mu_0 - E_0(\lambda)\mu_0 T_{abs}\big(\tau(\lambda),\mu_0\big) \\ &= E_0(\lambda)\mu_0\big(1 - T_{abs}(\tau(\lambda),\mu_0)\big) \end{aligned} \tag{15}$$

The amount of flux scattered out of the direct beam (into the upward and downward hemisphere) $E_{scat}(\lambda)$ can be computed as difference between the flux at the top the atmosphere, the flux absorbed by the atmosphere and that one absorbed out of the direct beam.

$$\begin{aligned} E_{scat}(\lambda) &= E_0(\lambda)\mu_0 - E_0(\lambda)\mu_0\big(1 - T_{abs}(\lambda,\mu_0)\big) \\ &\quad - E_0(\lambda)\mu_0 T_{abs}(\lambda,\mu_0) T_{scat}(\lambda,\mu_0) \\ &= E_0(\lambda)\mu_0 T_{abs}(\lambda,\mu_0)[1 - T_{scat}(\lambda,\mu_0)] \end{aligned} \tag{16}$$

Data for the extraterrestrial solar spectral irradiance $E_0(\lambda)$ are given by Fröhlich (1988)

Case b. *Single scattering diffuse model for a non reflecting surface.*

In this case the first and last terms of equation (12) are removed so we can write:

$$\begin{aligned} \mu \frac{dL(\lambda,\tau(\lambda),\mu'\varphi')}{d\tau(\lambda)} &= -\frac{\omega_0(\lambda)}{4\pi} E_0(\lambda) P(\lambda,\mu',\varphi';-\mu_0,\varphi_0)\,\cdot \\ &\quad \cdot \exp\left\{-\frac{\tau(\lambda)}{\mu_0}\right\} = J_{dir}(\lambda) \end{aligned} \tag{17}$$

The assumption to remove the first and third terms of equation (12) implies some errors; first of all an underestimation when largest values of scattering optical depths are involved. In such a case explicit treatment of the multiple scattering must be used.

In order to solve equation (17) we apply the following boundary conditions:

1. the downwelling diffuse radiance at the top of the atmosphere is:

$$L(\lambda,0,-\mu,\varphi) = 0 \tag{18}$$

2. the upwelling diffuse radiance at the surface is:

$$L(\lambda,\tau_0(\lambda),\mu,\varphi) = 0 \tag{19}$$

Then the solution for downwelling diffuse radiance at the surface is:

$$L(\lambda,\tau_0(\lambda),-\mu',\varphi') = \frac{\omega_0(\lambda)}{4\pi\mu}\int_0^{\tau_0(\lambda)} E_0(\lambda)P(\lambda,-\mu',\varphi';-\mu_0,\varphi_0)\cdot \cdot\exp\left\{-\frac{\tau(\lambda)}{\mu_0}\right\}d\tau(\lambda)$$

$$= \frac{\omega_0(\lambda)}{4\pi\mu}E_0(\lambda)P(\lambda,-\mu',\varphi';-\mu_0,\varphi_0)\mu_0\cdot \cdot\left[1-\exp\left\{-\frac{\tau_0(\lambda)}{\mu_0}\right\}\right] \quad (20)$$

and upwelling diffuse radiance at the top of atmosphere is:

$$L(\lambda,0,\mu',\varphi') = \frac{\omega_0(\lambda)}{4\pi\mu}\int_0^{\tau_0(\lambda)} E_0(\lambda)P(\lambda,\mu',\varphi';-\mu_0,\varphi_0)\cdot \cdot\exp\left\{-\frac{\tau(\lambda)}{\mu_0}\right\}d\tau(\lambda)$$

$$= \frac{\omega_0(\lambda)}{4\pi\mu}E_0(\lambda)\mu_0P(\lambda,\mu',\varphi';-\mu_0,\varphi)\cdot \cdot\left[1-\exp\left\{-\frac{\tau_0(\lambda)}{\mu_0}\right\}\right] \quad (21)$$

Then the downwelling diffuse spectral irradiance at the surface is obtained by integration of the radiance obtained by equation (20)

$$E_{down}(\lambda,\mu_0) = \int_0^{2\pi}\int_0^{-1} L(\lambda,\tau_0(\lambda),-\mu',\varphi')\mu'd\mu'd\varphi'$$

$$= \frac{\omega_0(\lambda)}{2}E_0(\lambda)\mu_0\left[1-\exp\left\{-\frac{\tau_0(\lambda)}{\mu_0}\right\}\right]\cdot \cdot\int_0^{-1} P(\lambda,-\mu',-\mu_0)d\mu' \quad (22)$$

and the upwelling diffuse spectral irradiance (exitance) is:

$$E_{up}(\lambda,\mu_0) = \int_0^{2\pi}\int_0^{1} L(\lambda,0,\mu',\varphi')\mu'd\mu'd\varphi'$$

$$= \frac{\omega_0(\lambda)}{2}E_0(\lambda)\mu_0\left[1-\exp\left\{-\frac{\tau_0(\lambda)}{\mu_0}\right\}\right]\cdot \cdot\int_0^{1} P(\lambda,\mu',-\mu_0)d\mu' \quad (23)$$

The integral of the phase function can be solved by the method of Gaussian quadrature (see for example Liou (1980))

Case c. ***Multiple scattering with surface reflectance***

Let us consider the case in which we have multiple scattering in atmosphere and a surface reflectance.

In such a case we remove the second term in equation (12). Thus it can be solved separating the radiance into upwelling and downwelling components with proper boundary conditions.

1. Upwelling radiance.

   Multiplying equation (12) by the integrating function $\exp\left\{-\frac{\tau(\lambda)}{\mu}\right\}$; dividing by μ and integrating both sides of the equation from $\tau_0(\lambda)$ to $\tau(\lambda)$ we get:

$$L(\lambda,\tau(\lambda),\mu',\varphi') = L(\lambda,\tau_0(\lambda),\mu',\varphi')\cdot\exp\left\{-\frac{\tau_0(\lambda)-\tau(\lambda)}{\mu}\right\} \quad (24)$$

$$+\int_0^{2\pi}\int_{\tau(\lambda)}^{\tau_0(\lambda)} J_{diff}(\lambda,\tau'(\lambda),\mu',\varphi')\exp\left\{-\frac{\tau'(\lambda)-\tau(\lambda)}{\mu}\right\}\frac{d\tau'}{\mu}d\mu'd\varphi'$$

   This equation describes the spectral radiance as measured by a downward looking observer located at optical depth $\tau(\lambda)$

2. Downwelling radiance.

   Following the procedure of upwelling radiance but integrating from 0 to $\tau(\lambda)$ we get:

$$L(\lambda,\tau(\lambda),-\mu,\varphi') = L(\lambda,0,-\mu',\varphi')\cdot\exp\left\{-\frac{\tau(\lambda)}{\mu}\right\} +\int_0^{2\pi}\int_0^{\tau(\lambda)} J_{diff}(\lambda,\tau'(\lambda),\mu',\varphi')\exp\left\{-\frac{\tau(\lambda)-\tau'(\lambda)}{\mu}\right\} \frac{d\tau'(\lambda)}{\mu}d\mu'd\varphi' \quad (25)$$

   with $0<\mu\leq 1$

In order to solve the integral equation it is necessary to specify the boundary conditions.

At the top of the atmosphere ($\tau(\lambda) = 0$) we have no diffuse radiance and only the direct solar radiation enters;

$$L_{diff}(\lambda, 0, -\mu, \varphi) = 0$$
$$L(\lambda, 0, -\mu, \varphi) = E_0(\lambda)\delta(-\mu, \mu_0)\delta(\varphi, \varphi_0) \quad (26)$$

The Dirac delta (δ) function makes this term is zero except for the sun direction (μ_0, φ_0). $E_0(\lambda)$ is the solar irradiance on a surface whose normal is in the direction of μ_0 and φ_0.

The boundary conditions at the surface are more complicated because of the surfa -flectance. Since the irradiation to the earth's surface is determined by the sum of the direct solar radiation and scattered radiation from all over the sky we can write:

$$E(\lambda, \tau_0(\lambda)) = E_0(\lambda)\mu_0 \exp\left\{-\frac{\tau_0(\lambda)}{\mu_0}\right\} + \int_0^{2\pi}\int_0^1 L(\lambda, \tau_0(\lambda), -\mu', \varphi')\mu' d\mu' d\varphi' \quad (27)$$

and hence

$$L(\lambda, \tau_0(\lambda), \mu', \varphi') = r(\lambda, \mu', \varphi'; -\mu_0; \varphi_0) \cdot E_0(\lambda)\mu_0 \cdot \exp\left\{-\frac{\tau_0(\lambda)}{\mu_0}\right\} + \int_0^{2\pi}\int_0^1 r(\lambda, \mu', \varphi', \mu, \varphi) \cdot L(\lambda, \tau_0(\lambda), -\mu', \varphi') \cdot \mu' d\mu' d\varphi' \quad (28)$$

where $r(\lambda, \mu', \phi', \mu_0, \phi_0)$ is the bidirectional reflectance distribution function which depends on the direction of the irradiating flux and the direction along which the reflected flux is detected.

Thus the integral equations (22) and (23) subject to the boundary condition (26) and (28), can be solved in order to provide a complete solution to the problem of radiative transfer in a plane-parallel, homogeneous atmosphere. We get:

1. Upwelling radiance

$$L(\tau(\lambda), \mu', \varphi') = \frac{\omega_0(\lambda)}{4\pi\mu}\int_{\tau(\lambda)}^{\tau_0(\lambda)} E_0(\lambda)\exp\left\{-\frac{\tau'(\lambda)}{\mu_0}\right\} \cdot$$

$$\cdot P(\lambda, \mu', \varphi'; -\mu_0, \varphi_0) \cdot \exp\left\{-\frac{\tau'(\lambda) - \tau(\lambda)}{\mu}\right\} d\tau'(\lambda)$$
$$+ \frac{\omega_0(\lambda)}{4\pi\mu}\int_{\tau(\lambda)}^{\tau_0(\lambda)}\int_0^{2\pi}\int_{-1}^{+1} P(\mu', \varphi'; \mu, \varphi)L(\lambda, \tau(\lambda), \mu', \varphi')d\mu' d\varphi' \cdot \exp\left\{-\frac{\tau'(\lambda) - \tau(\lambda)}{\mu}\right\} d\tau'(\lambda)$$
$$+ r(\lambda, \mu', \varphi'; -\mu_0, \varphi_0)E_0(\lambda)\exp\left\{-\frac{\tau_0(\lambda)}{\mu_0}\right\}\exp\left\{-\frac{\tau_0(\lambda) - \tau}{\mu}\right\}\mu_0$$
$$+ \int_0^{2\pi}\int_0^1 r(\lambda, \mu', \varphi'; \mu, \varphi) \cdot L(\lambda, \tau_0(\lambda); -\mu', \varphi') \cdot \exp\left\{-\frac{\tau_0(\lambda) - \tau(\lambda)}{\mu}\right\}\mu' d\mu' d\varphi' \quad (29)$$

In this equation the first term describes the radiation scattered out of the solar direct beam; the second term contributes to the multiplying of scattered photons; third and fourth terms are respectively the contribution of the direct and diffuse radiation reflected by the surface.

2. Downwelling radiance

$$L(\lambda, -\mu', \varphi') = \frac{\omega_0(\lambda)}{4\pi\mu}\int_0^{\tau(\lambda)} E_0(\lambda)P(\lambda, -\mu', \varphi', -\mu_0, \varphi_0) \cdot \exp\left\{-\frac{\tau'(\lambda)}{\mu_0}\right\}\exp\left\{-\frac{\tau(\lambda) - \tau'(\lambda)}{\mu}\right\} d\tau'(\lambda)$$
$$+ \frac{\omega_0(\lambda)}{4\pi}\int_0^{\tau(\lambda)}\int_0^{2\pi}\int_{-1}^{1} P(-\mu', \varphi'; \mu, \varphi)L(\lambda, \tau'(\lambda); \mu', \varphi') \cdot \exp\left\{-\frac{\tau(\lambda) - \tau'(\lambda)}{\mu}\right\} d\mu' d\varphi' d\tau'$$
$$+ E_0(\lambda)\delta(-\mu', -\mu_0)\delta(\varphi', \varphi_0)\exp\left\{-\frac{\tau(\lambda)}{\mu}\right\} \quad (30)$$

In this equation the first and second terms are respectively the scattered direct solar radiation and multiple scattered photons, while the third describes the attenuated solar direct radiation with an optical depth defined by the path from sun to airborne platform.

The Radiative Transfer Equation in integral form has no analytic solution. However several methods of solution exist. A complete overview of these methods have been treated in the book "Radiative transfer in scattering and absorbing atmosphere: standard computational procedures", edited by Lenoble, 1985.

However in subsequent paragraphs we derive approximate solution applied to selected case studies.

3.1.1 Atmospheric Transmittance and Phase Function

As already mentioned in this section, approximated methods of RTE solutions have been proposed by several authors. Our approximated numerical solutions recall them, but are different in the treatment of the optical depth or transmittance functions whose functional form will be defined in the following paragraphs.

a. *Functional form of the transmission function related to the gases and particles present in atmosphere.*

As is widely known, besides the major constituent like O_2 and N_2, the Earth's atmosphere is composed of water vapor, carbon dioxide, ozone, sulphur dioxide, hydrogen, hydrogen sulfide, helium, nitrogen compounds, methane, carbon dioxide, formaldeid and solid and liquid particulate matter.

Since gases and particulate matter are not spatially homogeneously distributed, standard atmospheres have been built up in order to simulate their actual altitude distribution as a function of latitude.

We use as reference the standard atmosphere proposed by Kneizys et al. (1983) in LOWTRAN-6.

In order to avoid the complexity of the electromagnetic mechanisms involved in atmosphere we introduce some simplification and parameterization in our computation.

Detailed calculations can be found in Goody (1964), in Kneizys et al. (1983).

As mentioned above, the attenuation function along the sun path, at wavelenght λ can be described by the transmittance function $T(\lambda)$

$$T(\lambda) = \Pi_i T_i(\lambda) \tag{31}$$

At altitude h the transmission function is

$$T(\lambda, h) = \Pi_i T_i(\lambda, h) = \exp\left\{-\frac{\sum_i \tau_i(\lambda, z)}{\mu}\right\} \tag{32}$$

If we know the optical thickness of the whole atmosphere, $\tau_0(\lambda)$, the dependence on height of the optical depth is

$$\tau_i(\lambda, z) = H_i(z)\,\tau_0(\lambda) \tag{33}$$

with

$$H_i(z) = \frac{\int_0^z \rho_i(z')dz'}{\int_0^{top} \rho_i(z')dz'} \tag{34}$$

where ρ_i is the density of the constituent i at height z'.

Since we have seen that molecules (R), aerosol (a), ozone (O_3) and water vapor (w) are the constituents affecting the solar radiation attenuation in the visible and near infrared, we describe them by a parameterization function depending on wavelength λ expressed in μm.

Then the molecular optical depth is :

$$\tau_R(\lambda, z) = H_R(z)\,8.8 \times 10^{-3}\,\lambda^{-4.15+0.2\lambda} \tag{35}$$

where

$$H_R = 1 - \exp(-0.1188\,z - 1.16 \times 10^{-3} z^2) \quad z\,(\mathrm{Km}) \tag{36}$$

as proposed by van Stokkom and Guzzi (1984).

Assuming the aerosol load in the atmosphere in the atmosphere is described by a Junge distribution, whose concentration varies exponentially as a function of altitude we get:

$$\tau_a(\lambda, z) = H_a(z)\alpha\lambda^{-\beta} \tag{37}$$

where α and β are the so called Angstrom parameters (see Guzzi (1984) for further details) with

$$H_a(z) = 1 - \exp\left\{-\frac{z}{H_p}\right\} \qquad (38)$$

where H_p is the scale height given by Penndorf ($H_p = 0.97 \div 1.4$ for the first 5 Km above the Earth's surface)

The ozone optical depth can be obtained by

$$\tau_{O_3}(\lambda, z) = H_{O_3}(z) 0.03 \exp\left\{-277(\lambda - 0.6)^2\right\} \qquad (39)$$

with

$$H_{O_3}(z) = 1 - \frac{1.0183}{1 + 0.0183 \exp\frac{z}{5}} \qquad (40)$$

as computed by the relation proposed by Lacis and Hansen (1974).

The water vapor optical depth is:

$$\tau_w(\lambda, z) = H_w(z) w A_J \exp\left\{-(\lambda - \lambda_J)^2 B_J\right\} \qquad (41)$$

with

$$H_w(z) = 1 - \exp(-0.639 z) \qquad (42)$$

as computed by the relation proposed by Reitan (1963).

In table 1 the values of A_J and B_J are shown as a function of wavelength . The water content $w(grcm^{-2})$ can be obtained as $w = \exp(0.29 + 0.0617 T_d)$ where T_d is the dew point temperature at the surface.

The remaining gases are assumed to be mixed and acting, as far as attenuation is concerned, as a single gas.

Thus the optical depth of the mixed gases is given by

$$\tau_{mg}(\lambda, z) = \left(\frac{0.3 K_g(\lambda) X_g(z)}{(1 + 25.25 K_g(\lambda) X_g(z))^{0.45}}\right) \qquad (43)$$

j	$\Delta\lambda_j(\mu m)$	$\lambda_j(\mu m)$	A_j	B_j
1	0.03	0.718	0.0315	8.60×10^3
2	0.03	0.810	0.0408	6.90×10^3
3	0.13	0.935	0.1393	0.66×10^3
4	0.20	1.130	0.1508	0.28×10^3
5	0.35	1.395	0.5447	0.13×10^3
6	0.54	1.870	0.3857	0.05×10^3

Table 1: Values of the parameters A_j and B_j

λ	k_g	λ	k_g
0.76	0.300E + 01	2.20	0.380E − 03
0.77	0.210E + 00	2.30	0.110E − 02
		2.40	0.170E − 03
1.25	0.730E − 02	2.50	0.140E − 03
1.30	0.400E − 03	2.60	0.660E − 03
1.35	0.110E − 03	2.70	0.100E + 03
1.40	0.100E − 04	2.80	0.150E + 03
1.45	0.640E − 01	2.90	0.130E + 00
1.50	0.630E − 03	3.00	0.950E − 02
1.55	0.100E − 01	3.10	0.100E − 02
1.60	0.640E − 01	3.20	0.800E + 00
1.65	0.145E − 02	3.30	0.190E + 01
1.70	0.100E − 04	3.40	0.130E + 01
1.75	0.100E − 04	3.50	0.750E − 01
1.80	0.100E − 04	3.60	0.100E − 01
1.85	0.145E − 03	3.70	0.195E − 02
1.90	0.710E − 02	3.80	0.400E − 02
1.95	0.200E + 01	3.90	0.290E + 00
2.00	0.300E + 01	4.00	0.250E − 01
2.10	0.240E + 00		

Table 2: Effective absorption coefficients of uniformly mixed gases, km^{-1}

where $X_g(z)$ is the pathlength for the uniformly mixed gases expressed in km. X_g can be computed by the following polynomial best fit as function of z:

$$X_g(z) = -4.65 + 1.07z - 7.17z^2 + 2.47z^3 - 4.42z^4 + 3.91z^5 - 1.35z^6 \quad (44)$$

obtained by relation proposed by Leckner (1978) for the mixed gases.

Values of the effective coefficients K_g are shown as a function of wavelenghts in Table 2.

b. *The Phase Function.*

The phase function can be computed considering it as sum of the molecular phase function $P_R(\Omega)$ and aerosol phase function $P_a(\Omega)$.

The molecular phase function is defined by:

$$P_R(\Omega) = \frac{3}{4}(1 + \cos^2\Omega) \quad (45)$$

and the aerosol phase function is given by the Henyey - Greenstein function

$$P_a(\Omega) = \frac{1 - g^2}{(1 + g^2 - 2g\cos\Omega)^{3/2}} \quad (46)$$

where g depends on the types of aerosol present in the atmosphere.

In fig. 2 the Henyey-Greenstein phase function for different values of the anisotropy parameter η is shown.

Assuming the aerosol size distribution constant along the vertical phase function for an atmospheric layer lying between z_1 and z_2 altitudes we can express the total phase function as:

$$P(\Omega, z_1, z_2) = \frac{P_R(\Omega)[\tau_R(\lambda, z_2) - \tau_R(\lambda, z_1)] + P_a(\Omega)[\tau_a(\lambda, z_2) - \tau_a(\lambda, z_1)]}{[\tau_R(\lambda, z_2) - \tau_R(\lambda, z_1)] + [\tau_a(\lambda, z_2) - \tau_a(\lambda, z_1)]} \quad (47)$$

provided that the aerosol profile is known (see for instance Guzzi (1988)).

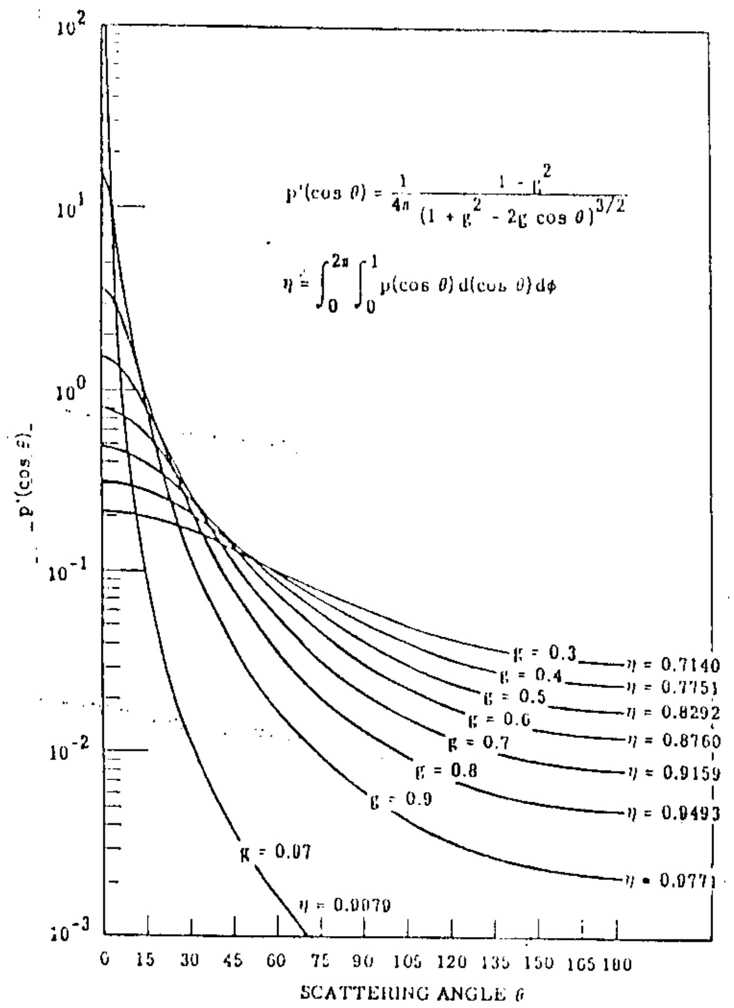

Fig. 2 Henyey - Greenstein phase function for different values of the anisotropy parameter η (after Turner, 1973)

3.1.2 Approximate method for the solution of the RTE in the visible and near infrared

Among the methods used by several authors we select the similarity principle, with whose aid the anisotropic scattering may be approximately reduced to isotropic scattering (Sobolev, 1963). As we have seen, the radiation field in the atmosphere is determined by the phase function $P(\Omega)$, optical depth $\tau(\lambda)$ and single scattering albedo $\omega_0(\lambda)$. A change in this quantity produces a change in the radiation field. The problem is to reduce the anisotropic scattering to the simpler isotropic case, without changing the atmospheric field.

The approximate similarity of the radiation field in the atmosphere with anisotropy scattering to the corresponding field in an atmosphere with isotropic scattering will take place only with large optical depth $\tau(\lambda)$ and pure scattering ($\omega_0 = 1$). In such a case we must average the radiation field over the azimuth since for isotropic scattering the radiance does not depend on the azimuth.

Then we develop approximate methods of solution with sufficient flexibility for adaption to any practical situation. So in the case of conservative cases of perfect scattering i.e. $\omega_0 = 1$ in semi-infinite plane parallel atmosphere the Radiative Transfer Equation can be written:

$$\begin{aligned}\mu\frac{dL(\tau,\mu,\varphi)}{d\tau} &= L(\tau,\mu,\varphi)\\ &- \frac{1}{4\pi}\int_{-1}^{+1}\int_0^{2\pi} P(\mu,\varphi;\mu',\varphi')L(\tau,\mu',\varphi')d\mu',d\varphi' \quad (48)\end{aligned}$$

The dependence over the wavelength has been omitted. Multiplying this equation by μ and integrating overall solid angle we have:

$$\begin{aligned}&\frac{d}{d\tau}\int_{-1}^{+1}\int_0^{2\pi} L(\tau,\mu,\varphi)\mu^2 d\mu d\varphi = \int_{-1}^{+1}\int_0^{2\pi} L(\tau,\mu,\varphi)\mu d\mu d\varphi\\ &-\frac{1}{4\pi}\int_{-1}^{+1}\int_0^{2\pi} d\mu' d\varphi L(\tau,\mu',\varphi')\int_{-1}^{+1}\int_0^{2\pi} d\mu d\varphi \mu P(\mu,\varphi;\mu'\varphi') \quad (49)\end{aligned}$$

where the net flux integral $\int_{-1}^{+1}\int_0^{2\pi} L(\tau,\mu,\varphi)\mu d\mu d\varphi = \pi F$ with F = constant. Let us suppose that the phase function can be expanded in Legendre

Polynomials. Then:

$$P(\mu,\varphi;\mu',\varphi') = \sum_{e=0}^{N}\omega_e P_e[\mu\mu' + (1-\mu^2)^{\frac{1}{2}}(1-\mu'^2)^{\frac{1}{2}}\cos(\varphi-\varphi')] \quad (50)$$

Expanding P_e by the addition theorem for spherical harmonics we find:

$$P(\mu,\varphi;\mu'\varphi) = \sum_{m=0}^{N}\sum_{e=m}^{N}\varpi_e^m P_e^m(\mu)P_e^m(\mu')\cos m(\varphi-\varphi') \quad (51)$$

where

$$\omega_e^m = (2-\delta_{0,m})\omega\frac{(e-m)!}{(e+m)!}$$
$$e = m,\ldots N 0 \le m \le N$$
$$\delta_{0,m} = \{^1_0$$

and for $e = 1$ and $m = 0$ corresponding to the azimuth independence case we obtain:

$$\frac{1}{4\pi}\int_{-1}^{+1}\int_0^{2\pi} P(\mu,\varphi;\mu',\varphi')\mu d\mu d\varphi = \frac{1}{2}\omega_1\mu'\int_{-1}^{+1}\mu^2 d\mu = \frac{1}{3}\omega_1\mu' \quad (52)$$

where $\omega_e = \omega_1$ and $P_1(\mu) = \mu$ for the first order of the Legendre polynomials. Hence the equation (49) reduces to:

$$\frac{1}{4\pi}\frac{d}{d\tau}\int_{-1}^{+1}\int_0^{2\pi} L(\tau,\mu,\varphi)\mu^2 d\mu d\varphi = \frac{1}{4}(1-\frac{1}{3}\omega_1)F \quad (53)$$

Now writing:

$$K(\tau) = \frac{1}{4\pi}\int_{-1}^{+1}\int_0^{2\pi} L(\tau,\mu,\varphi)\mu^2 d\mu d\varphi \quad (54)$$

we have

$$\frac{dK}{d\tau} = \frac{1}{4}(1-\frac{1}{3}\omega_1)F$$

or, since F is constant we obtain the K integral

$$K = \frac{1}{4}F[(1-\frac{1}{3}\omega_1)\tau + c \quad (55)$$

where c is a constant.

Then in the conservative case the solution is:

$$L(\tau,\mu) = const\left(\tau + \frac{\mu}{1-\frac{1}{3}\omega_1}\right) \qquad (56)$$

that normalized to yield a net flux πF gives:

$$L(\tau,\mu) = \frac{3}{4}F\left[\left(1-\frac{1}{3}\omega_1\right)\tau + \mu\right] \qquad (57)$$

Irvine (1968)has demonstrated the applicability of the K integral to anisotropic-scattering problem, finding good agreement with exact methods when the atmosphere is thick.

His result for the quasi-isotropic case is:

$$K \cong \frac{1}{3}\overline{L} \qquad (58)$$

with

$$\overline{L} = \frac{1}{4\pi}\int_0^{2\pi}\int_{-1}^{+1} L(\tau,\mu,\varphi)d\mu d\varphi$$

obtained averaging over all space.

This solution fails for near - boundary conditions.

Another method has been developed by Turner (1973) starting from the very well known Schuster (1905) and Schwarzschild (1906) method.

Providing that for isotropic scattering the source function is azimuth independent, equation (48) can be written as:

$$\mu\frac{dL(\tau,\mu)}{d\tau} = L(\tau,\mu) - \frac{1}{2}\int_{-1}^{+1} L(\tau,\mu')d\mu' p(\mu,\mu') \qquad (59)$$

where

$$p(\mu,\mu') = \frac{1}{2\pi}\int_0^{2\pi} P(\mu,\varphi;\mu'\varphi')d\varphi' = 1$$

Dividing the radiation field into upward $L+$ and downward $L-$ stream of radiance, equation (59) can be divided into a pair of equations:

$$\begin{aligned}\frac{1}{2}\frac{dL_+(\tau)}{d\tau} &= L_+(\tau) - \frac{1}{2}(L_+(\tau) + L_-(\tau)) \\ -\frac{1}{2}\frac{dL_-(\tau)}{d\tau} &= L_-(\tau) - \frac{1}{2}(L_+(\tau) + L_-(\tau))\end{aligned} \qquad (60)$$

The solution of equation, subject to the usual boundary conditions ($L_- = 0$, at $\tau = 0$ for example), provides a first approximation. The crude two stream approximation suggests, nevertheless, visualization of the radiation field in terms of discrete streams.

At this point we assume to integrate over the hemisphere instead of the overall space like in the preceding method. Thus

$$\begin{aligned}L_+(\tau) &= \int_0^{2\pi}\int_0^1 L(\tau,\mu,\varphi)d\mu d\varphi \\ L_-(\tau) &= \int_0^{2\pi}\int_{-1}^0 L(\tau,\mu,\varphi)d\mu d\varphi\end{aligned} \qquad (61)$$

and as a weighted average

$$\begin{aligned}E_+(\tau) &= \int_0^{2\pi}\int_0^1 \mu L(\tau,\mu,\varphi)d\mu d\varphi \\ E_-(\tau) &= \int_0^{2\pi}\int_{-1}^0 \mu L(\tau,\mu,\varphi)d\mu d\varphi\end{aligned} \qquad (62)$$

that in a nearly isotropic field gives:

$$E_+ = \frac{1}{2}L_+$$
$$E_- = \frac{1}{2}L_-$$

Since the case to be solved is defined by the following equation:

$$\mu\frac{dL(\tau)}{d\tau} = L(\tau,\mu,\varphi) - \frac{1}{4\pi}\int_0^{2\pi}\int_{-1}^{+1} P(\mu,\varphi;\mu',\varphi')L(\tau,\mu',\varphi')d\mu d\varphi - \frac{E_0(\tau)}{4\pi}P(\mu,\varphi;-\mu_0,\varphi_0) \qquad (63)$$

that is equation (12) in the solar field, we make the following assumptions on the atmosphere and surface.

a. The atmosphere is homogeneous conservative, plane parallel, with no absorption

b. No clouds exist

c. The surface albedo is spatially constant (Lambertian surface)

If the phase function can be represented by the forward and backward components, we can write it by two delta functions as:

$$
\begin{aligned}
P(\mu,\varphi;\mu',\varphi') &= F\delta(\mu-\mu')\delta(\varphi-\varphi') \\
&+ B\delta(\mu-\mu')\delta(\pi+\varphi-\varphi')
\end{aligned} \tag{64}
$$

where F and B are respectively the constant describing the amount of scattering in the forward and backward direction respectively.

Since as we have seen the phase function is normalized to the unity

$$\frac{F}{4\pi}+\frac{B}{4\pi}=1 \tag{65}$$

We can describe the fraction of the total radiation scattered into a forward hemisphere by

$$\eta=\frac{F}{4\pi}$$

and

$$\frac{B}{4\pi}=1-\eta$$

Inserting equations (64) and (65) into equation (63) we get:

$$
\begin{aligned}
\mu\frac{dL(\tau)}{d\tau} &= (1-\eta)[L(\tau,\mu,\varphi)-L(\tau,-\mu,\pi+\varphi)] \\
&- \eta E_0(\tau)\delta(\mu+\mu_0)\delta(\varphi-\varphi_0) \\
&- (1-\eta)E_0(\tau)\delta(\mu-\mu_0)\delta(\pi+\varphi-\varphi_0)
\end{aligned} \tag{66}
$$

We define the radiation field as:

$$
\begin{aligned}
L(\tau,\mu,\varphi) &= \frac{1}{\mu_0}[E'_+(\tau)\delta(\mu-\mu_0)\delta(\pi+\varphi_0-\varphi) \\
&+ E'_-(\tau)\delta(\mu+\mu_0)\delta(\varphi-\varphi_0)
\end{aligned} \tag{67}
$$

where $E_+(\tau)$ and $E_-(\tau)$ are the upward and downward irradiance in the positive and negative directions, respectively.

Inserting equation number (66) into equation (67) we obtain a couple of linear differential equations

$$
\begin{aligned}
\frac{dE'(\tau)}{d\tau} &= \frac{(1-\eta)}{\mu_0}[E'_+(\tau)-E'_-(\tau)]-(1-\eta)E_0(\tau) \\
-\frac{dE'(\tau)}{d\tau} &= \frac{(1-\eta)}{\mu_0}[E'_-(\tau)-E'_+(\tau)]-\eta E_0(\tau)
\end{aligned} \tag{68}
$$

Let us assume the surface albedo is zero, then the boundary conditions are:

$$E'_+(\tau_0)=E'_-(0)=0$$

then the solution of equation (65) is:

$$
\begin{aligned}
E'_+(\tau) &= \frac{\mu_0E_0(1-\eta)(\tau_0-\tau)}{\mu_0+(1-\eta)\tau_0} \\
E'_-(\tau) &= \mu_0E_0[\frac{\mu_0+(1-\eta)(\tau_0-\tau)}{\mu_0+(1-\eta)\tau_0}\}\cdot\exp\left\{-\frac{\tau}{\mu_0}\right\}] \\
\tilde{E}'_-(\tau) &= \mu_0E_0[\frac{\mu_0+(1-\eta)(\tau_0-\tau)}{\mu_0+(1-\eta)\tau_0}]
\end{aligned}
$$

where $E'_+(\tau)$ is the upward diffuse irradiance; $E'_-(\tau)^+$ is the downward diffuse irradiance and $\tilde{E}'_-$ is the total (diffuse + direct) downward irradiance.

If we have not the solar input, equation (63) can be written:

$$
\begin{aligned}
\mu\frac{dL}{d\tau} &= L(\tau,\mu,\varphi) \\
&- \frac{1}{4\pi}\int_0^{2\pi}\int_{-1}^{1}P(\mu,\varphi;\mu',\varphi')L(\tau,\mu',\varphi)d\mu'd\varphi'
\end{aligned} \tag{69}
$$

that multiplied by $d\mu d\varphi$ and integrated by the limits $0\le\mu<1;0<\varphi\le2\pi$ and $-1<\mu\le0;0<\varphi\le2\pi$ gets:

$$
\begin{aligned}
\frac{dE"_+(\tau)}{d\tau} &= (1-\eta)[L_+(\tau)-L_-(\tau)] \\
\frac{dE"_-(\tau)}{d\tau} &= (1-\eta)[L_+(\tau)-L_-(\tau)]
\end{aligned}
$$

with the same notation quoted before (eqs. (61) (62)).
When the field is isotropic:

$$E"_+(\tau) = \frac{1}{2} L_+(\tau)$$
$$E"_-(\tau) = \frac{1}{2} L_-(\tau) \qquad (70)$$

that differentiated and inserted into equation (69) give:

$$\frac{dE"_+(\tau)}{d\tau} = 2(1-\eta)[E"_+(\tau) - E"_-(\tau)]$$
$$\frac{dE_-(\tau)}{d\tau} = 2(1-\eta)[E"_+(\tau) - E"_-(\tau)] \qquad (71)$$

Since the boundary conditions for reflecting surface are:

$$E"_-(0) = 0$$
$$E"_+(\tau_0) = rE'(\tau_0)$$

the differential equation (71) has the solution:

$$E"_+(\tau) = \frac{r\mu_0^2 E_0}{\mu_0 + (1-\eta)\tau_0}\left[\frac{1+2(1-\eta)\tau}{1+2(1-\eta)\tau_0}\right]$$
$$E"_-(\tau) = \frac{r\mu_0^2 E_0}{\mu_0 + (1-\eta)\tau_0}\left[\frac{2(1-\eta)\tau}{1+2(1-\eta)\tau_0}\right] \qquad (72)$$

where r is the function describing the reflection from the surface.

We find the complete irradiance by adding the case of solar generated anisotropic field to those for reflected isotropic field.

Then we obtain for upward irradiance:

$$E_+(\tau) = \frac{\mu_0 E_0}{\mu_0 + (1-\eta)\tau_0}\left[(1-\eta)(\tau_0 - \tau) + r\mu_0 \frac{1+2(1-\eta)\tau}{1+2(1-\eta)\tau_0}\right] \qquad (73)$$

and for downward irradiance:

$$E_-(\tau) = \frac{\mu_0 E_0}{\mu_0 + (1-\eta)\tau_0}\left[\mu_0 + (1-\eta)(\tau_0 - \tau) - [\mu_0 + (1-\eta)]\exp\left\{-\frac{\tau}{\mu_0}\right\} + \frac{2r\mu_0(1-\eta)\tau}{1+2(1-\eta)\tau_0}\right] \qquad (74)$$

The total downward irradiance is:

$$\tilde{E}_-(\tau) = \frac{\mu_0 E_0}{\mu_0 + (1-\eta)\tau_0} \cdot \left[\mu_0 + (1-\eta)(\tau_0 - \tau) + \frac{2r\mu_0(1-\eta)\tau}{1+2(1-\eta)\tau_0}\right] \qquad (75)$$

In order to avoid $\tilde{E}_-(\tau)$ exceeding by a certain value of r, η, μ_0 and τ_0 the value of $\mu_0 E_0$ we put the condition that:

$$\eta \leq 1 + \frac{1 - 2r\mu_0}{2\tau_0}$$

Then the radiance can be found by using the following approximation:

$$L(\tau,\mu,\varphi) = \frac{1}{\mu_0}[E'_+(\tau)\delta(\mu - \mu_0)\delta(\pi + \varphi_0 - \varphi) + E'_-(\tau)\delta(\mu + \mu_0)\delta(\varphi - \varphi_0)] + \frac{E"_+(\tau) + E"_-(\tau)}{\pi} \qquad (76)$$

where the combination of delta function represents the solar generated anisotropic field, and the last term is the radiation field reirradiated from the surface.

Then the upwelling radiance (path radiance $L_p(\tau,\mu,\varphi)$ can be obtained by using equation (76):

$$L_p(\tau,\mu,\varphi) = \frac{E_0}{4\pi(\mu_0 + (1-\eta)\tau_0)}\Big(\{(1-\eta)\tau_0[P(\mu,\varphi,\mu_0,\pi+\varphi_0) + P(\mu,\varphi;-\mu_0,\varphi_0)] + \mu_0 P(\mu,\varphi;-\mu_0,\varphi_0) + \frac{4\mu_0^2 r}{1+2(1-\eta)\tau_0}\}\left[1 - \exp\left\{-\frac{\tau_0 - \tau}{\mu}\right\}\right] + \Big\{(1-\eta)\Big[(P(\mu,\varphi;\mu_0,\pi+\varphi_0) + P(\mu,\varphi,-\mu_0,\varphi_0)\Big]$$

$$
- \frac{16(1-\eta)\mu_0^2 r}{1+2(1-\eta)\tau_0}\Big\} \cdot \Big[(\tau_0 + \mu)\exp\Big\{-\frac{(\tau_0-\tau)}{\mu}\Big\} - (\tau+\mu)\Big]\Big) \tag{77}
$$

The downwelling radiance or sky radiance L_s will be:

$$
\begin{aligned}
L_S(\tau,-\mu,\varphi) = & \frac{E_0}{4\pi(\mu_0+(1-\eta)\tau_0)}\Big(\Big\{(1-\eta)\tau_0[P(-\mu,\varphi;\mu_0,\pi+\varphi_0) \\
& + P(-\mu,\varphi;-\mu_0,\varphi_0)] + \mu_0 P(-\mu,\varphi;-\mu_0,\varphi_0) \\
& + \frac{4\mu_0^2 r}{1+2(1-\eta)\tau_0}\Big\} \cdot \Big(1-\exp\Big\{-\frac{\tau}{\mu}\Big\}\Big) \\
& - \Big\{(1-\eta)[P(-\mu,\varphi;\mu_0,\pi+\varphi_0) + P(-\mu,\varphi;-\mu_0,\varphi_0)] \\
& - \frac{16(1-\eta)\mu_0^2 r}{1+2(1-\eta)\tau_0}\Big\}\Big(\mu\exp\Big\{-\frac{\tau}{\mu}\Big\} + \tau - \mu\Big)\Big)
\end{aligned} \tag{78}
$$

with the followings phase functions:

$$
\begin{aligned}
P(\mu,\varphi;\mu_0,\pi+\varphi_0) &= P[\mu\mu_0 - \sqrt{(1-\mu^2)(1-\mu_0^2)}\cos(\varphi-\varphi_0)] \\
P(\mu,\varphi;-\mu_0,\varphi_0) &= P[-\mu\mu_0 + \sqrt{(1-\mu^2)(1-\mu_0^2)}\cos(\varphi-\varphi_0)] \\
P(-\mu,\varphi;\mu_0,\pi+\varphi_0) &= P[-\mu\mu_0 - \sqrt{(1-\mu^2)(1-\mu_0^2)}\cos(\varphi-\varphi_0)] \\
P(-\mu,\varphi;-\mu_0,\varphi_0) &= P[\mu\mu_0 + \sqrt{(1-\mu^2)(1-\mu_0^2)}\cos(\varphi-\varphi_0)]
\end{aligned}
$$

In order to calculate the irradiance $E_+(\tau), E_-(\tau), \bar{E}$ we need to define the optical depth τ, the optical thickness τ_0, the anisotropy parameter η, the albedo r and the solar zenith angle μ_0 (λ has been omitted).

A three dimensional plot, based on Elterman (1970) work, of the relationship between optical depth τ, altitude h and visual range v (in km) is shown in fig. 3.

Measurements of one of the three parameters permit us to compute the other two; the parameter η is given, in the approximation used by:

$$
\eta = \frac{0.5\tau_{mol} + 0.95\tau_{aerosol}}{\tau_{mol} + \tau_{aerosol}}
$$

Then the dependence of irradiance on the altitude, from the prescribed parameters r, λ, μ are calculated and shown in fig. 4 and 5 for two different visual ranges.

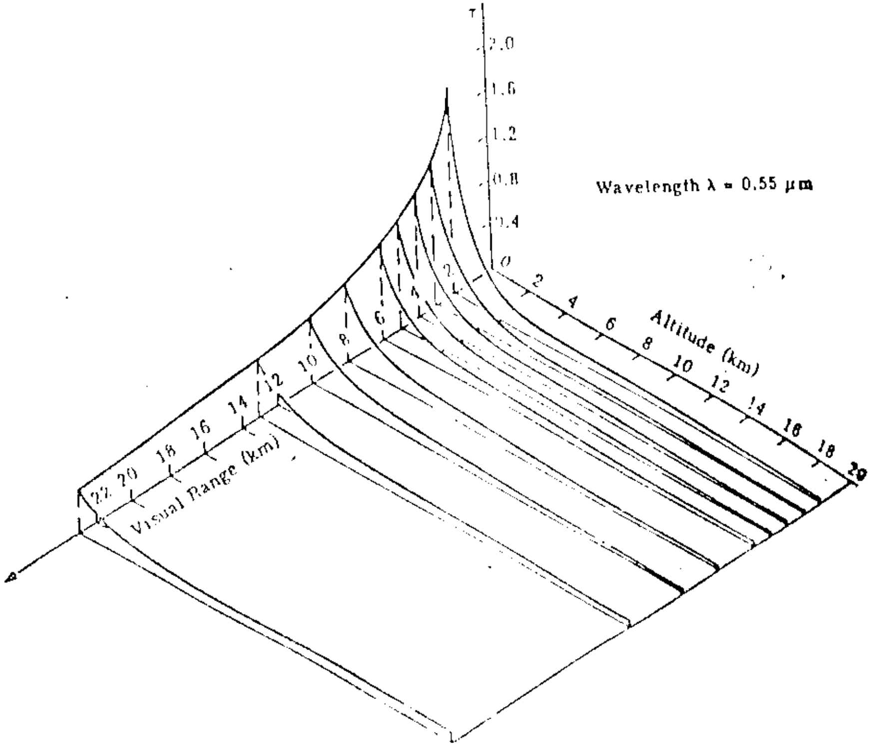

Fig. 3 Optical depth versus visual range and altitude (after Turner, 1973)

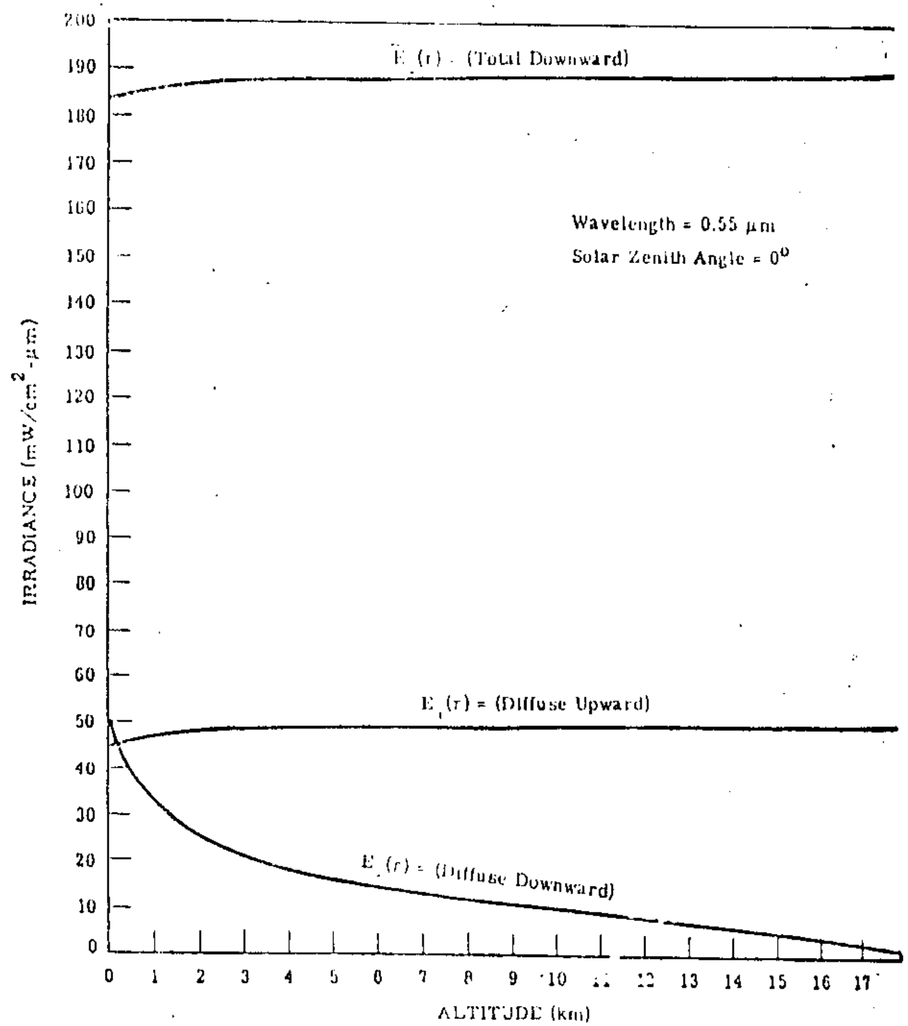

Fig. 4 Dependence of irradiance on altitude with visual range = 23 km and surface albedo = 0.25 (after Turner, 1973)

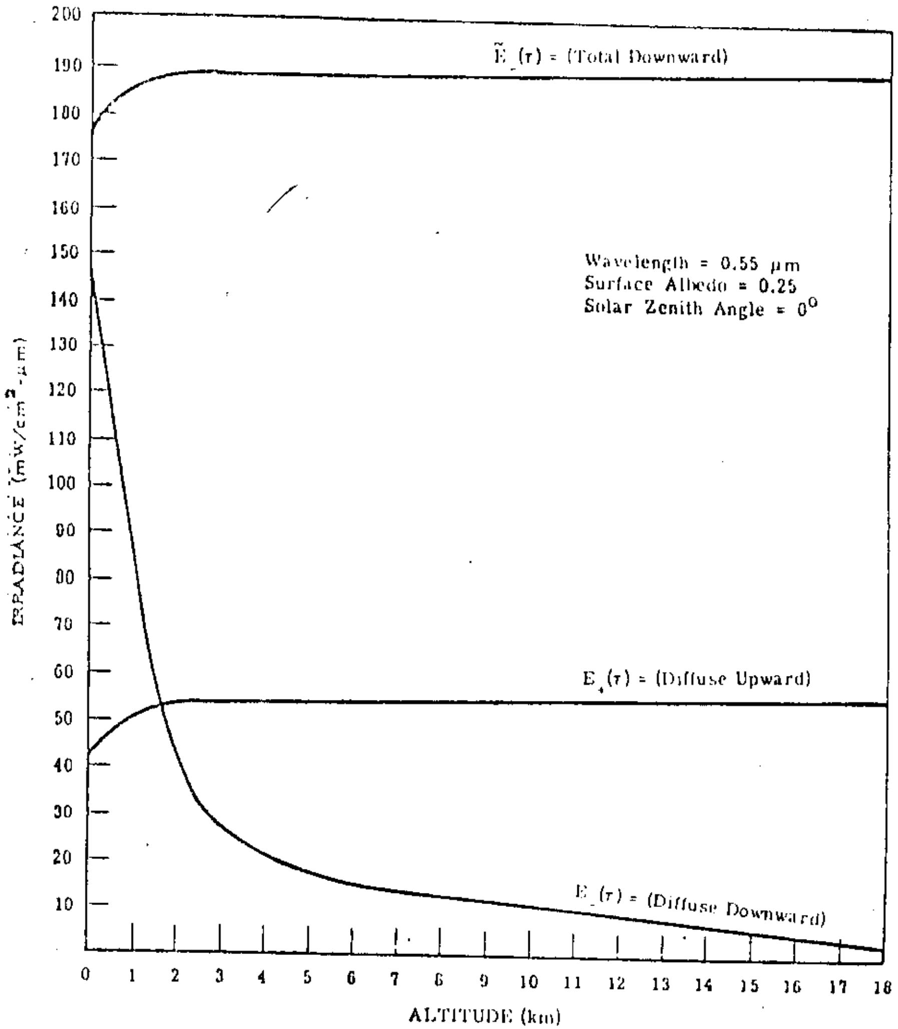

Fig. 5 as Fig. 4 visual range = 2 km and surface albedo = 0.25 (after Turner, 1973)

The sky and the path radiance versus zenith scan angle are shown in fig. 6 and 7 and the sky and path radiance as a function of a zenith scan angle and visual range are shown in fig. 8 and 9.

3.2 Longwave Radiation Transfer in Clear Atmosphere

Since in the infrared spectrum scattering processes are negligible we can remove, from the equation (11), the corresponding source functions from RTE and write:

$$\mu\frac{dL(\lambda,\tau,\Omega)}{d\tau} = L(\lambda,\tau,\Omega) - J_e(\lambda,T^*)$$
$$= +L(\lambda,\tau,\Omega) - \Big(1-\omega_0(\lambda)\Big)B(\lambda,T^*) \qquad (79)$$

This equation can be easily solved with the boundary condition where the Earth's surface is described by its thermal emission in terms of Planck's function $B(\lambda,T_s^*)$ depending on the surface temperature T_s^* multiplied by the spectral emittance $\Big(1-\omega_0(\lambda)\Big)=\epsilon(\lambda)$ Then the solutions are:

1. Upwelling radiance.

   It is given by multiplying the integrating function $\exp\left(-\frac{\tau}{\mu}\right)$, dividing by μ and integrating from $\tau_0(\lambda)$ to $\tau(\lambda)$

$$L(\lambda,\tau(\lambda),\mu,\varphi) = \epsilon(\lambda)B(\lambda,T_s^*)\exp\left\{-\frac{\tau_0(\lambda)-\tau(\lambda)}{\mu}\right\}$$
$$+\frac{1-\omega_0(\lambda)}{\mu}\int_{\tau(\lambda)}^{\tau_0(\lambda)} B\Big(\lambda,T^*\big(\tau'(\lambda)\big)\Big)\exp\left\{-\frac{\tau'(\lambda)-\tau(\lambda)}{\mu}\right\}d\tau'(\lambda) \qquad (80)$$

   where the first term describes the emission from a grey surface of temperature T_s^* and the second term the emission of the atmosphere.

2. Downwelling radiance.

   It is given by integrating equation (79) from 0 to $\tau(\lambda)$

$$L\Big(\lambda,\tau(\lambda),\ \mu,\varphi\Big) = \frac{1-\omega_0(\lambda)}{\mu}\int_0^{\tau(\lambda)} B\Big(\lambda,T^*\big(\tau'(\lambda)\big)\Big)\cdot$$
$$\cdot\exp\left\{-\frac{\tau(\lambda)-\tau'(\lambda)}{\mu}\right\}d\tau'(\lambda) \qquad (81)$$

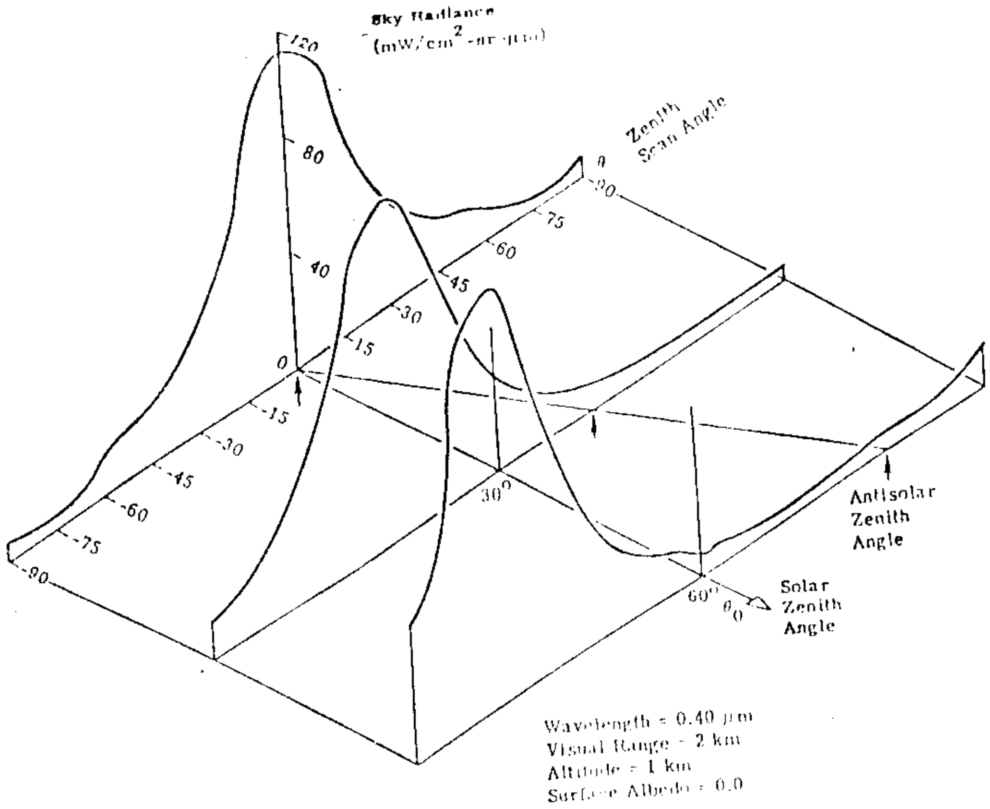

Fig. 6 Sky radiance versus scan angle and solar zenith angle (after Turner, 1973)

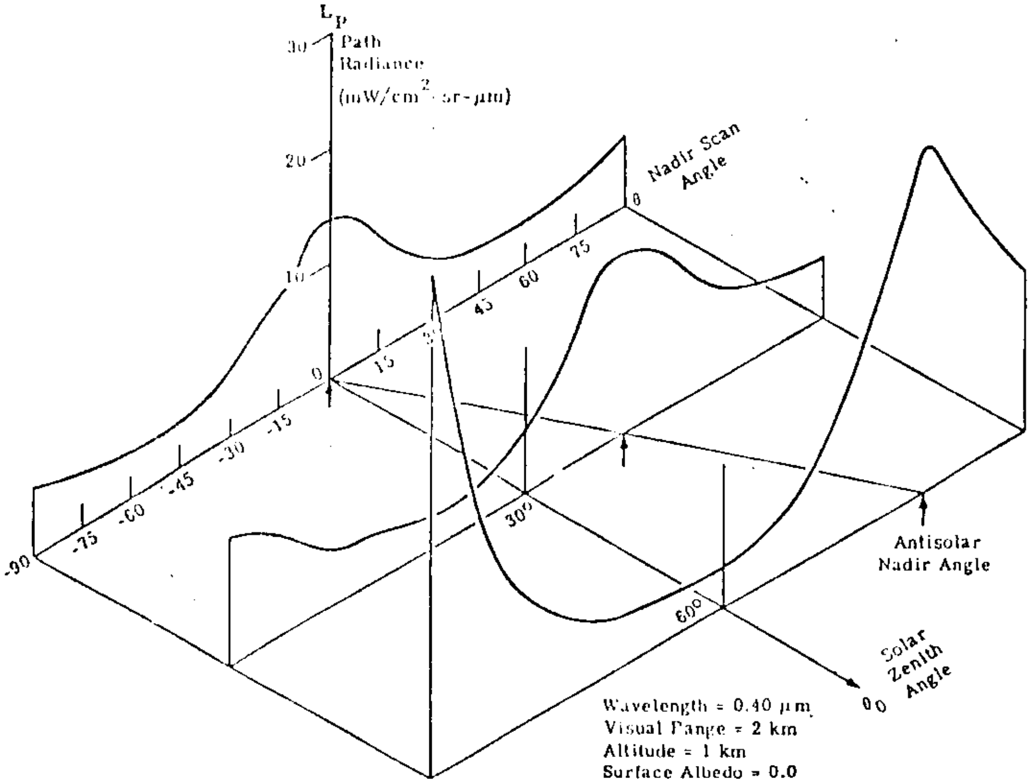

Fig. 7 Path radiance versus scan angle and solar zenith angle (after Turner, 1973)

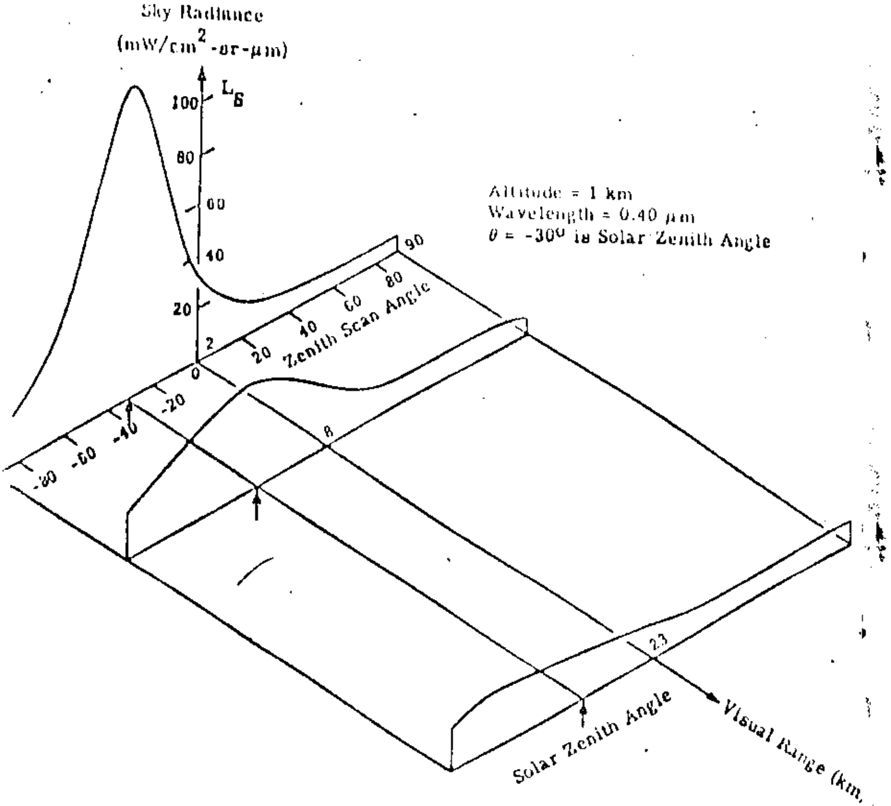

Fig. 8 Sky radiance versus zenith scan angle and visual range (after Turner, 1973)

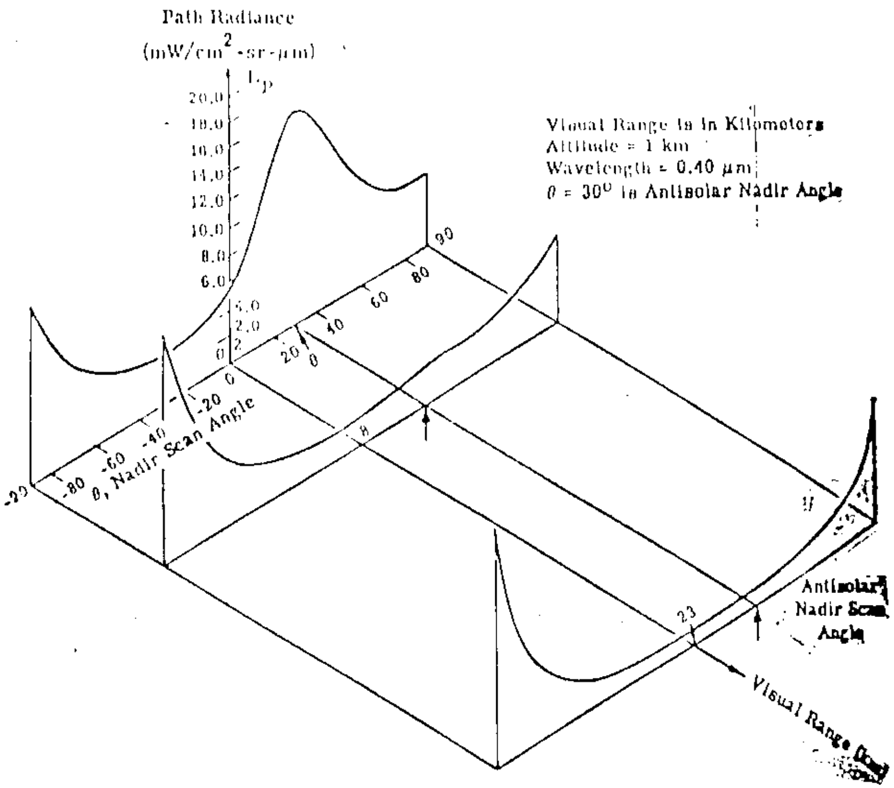

Fig. 9 Path radiance versus nadir scan angle and visual range (after Turner, 1973)

which describes the emission of the atmosphere.

Solutions of the integral equations will be given in subsequent paragraphs. They can be also found in Platt and Paltridge (1976), and Liou (1980).

3.2.1 Solution of the Radiative Transfer Equation in the infrared

The solution of equation (80) and (81) is determined by the knowledge of the transmittance function in the infrared.

The first term of equation (80) is the radiance emitted at the surface and reaching $\tau(\lambda)$ while the second term is the integrated contribution at $\tau'(\lambda)$ from each atmospheric slab along $\frac{\tau_0(\lambda)-\tau(\lambda)}{\mu}$.

A simple interpretation can be found if we see fig. 10 in which the atmosphere is plane - stratified and the ground has $\varepsilon = 1$. Then we can simplify the upwelling radiance given by equation (80) as follows:

$$L(\lambda, z, \mu) = B(\lambda, T_s^*)\exp\left\{-\frac{\tau_0(\lambda)}{\mu}\right\} + \int_{z_0}^{z} B(\lambda, T_{z'}^*)\exp\left\{-\frac{\tau'(\lambda)}{\mu}\right\}\frac{K(\lambda)\rho(z')}{\mu}dz' \qquad (82)$$

providing the atmosphere is a black body.

The downwelling radiance given by equation (81) is then:

$$L(\lambda, z, -\mu) = = \frac{1}{\mu}\int_{z_0}^{z} B(\lambda, T_{z'}^*)\exp\left\{-\frac{\tau'(\lambda)}{\mu}\right\}K(\lambda)\rho(z')dz' \qquad (83)$$

where:

$$\tau'(\lambda) = \tau(\lambda, z, z') = \int_{z}^{z'} K(\lambda)\rho(z'')dz''$$

The exponentials of the equations are the transmittances which have the following derivative:

$$\frac{dT(\lambda, z, z', \mu)}{dz'} = \exp\left\{-\frac{\tau'(\lambda)}{\mu}\right\}\frac{K(\lambda)\rho(z')}{\mu}$$

4 Applications of Radiative Transfer Equation to selected case study

4.1 Introduction to the problems of the Radiative transfer processes measured in the visible and near infrared by a flying platform

Passive remote sensing in the visible and near infrared utilizes the spectral solar radiation interacting with the surface and with the atmospheric constituents and that leave scattered signatures which can be used for the identification of the spatial features or many bodies (vegetation index; water leaving radiance; aerosol load).

The radiance measured by a sensor mounted on a satellite is given by the sum of the solar direct and diffuse spectral radiation reflected by the surface and the path radiance (all the terms have been described in Chapter 3).

These components are shown in fig. 18.

The radiance measured can be written as:

$$L(\lambda) = L_p(\lambda) + L_{sung}(\lambda) + L_{skyg}(\lambda) \qquad (119)$$

where $L_p(\lambda)$ is the path radiance, that is the cumulative radiance scattered into the field of view of the sensor by the atmospheric constituents. $L_{sung}(\lambda)$ is the sun glitter radiance , that is the direct radiance reflected by the surface into the field of view of the sensor. $L_{skyg}(\lambda)$ is the sky glitter radiance, that is the diffuse sun radiance reflected by the surface into the field of view of the sensor.

The algorithms which describe the path radiance, the sky glitter radiance and the sun glitter radiance have been obtained by the solutions of the Radiative Transfer Equation as presented in Chapter 3.

Assuming the absorption and scattering processes are independent, the atmospheric processes can be simply described by the optical thickness $\tau(\lambda)$ as sum of the scattering and absorbing processes.

The sky and sun glitter radiance are the sun and sky spectral radiance respectively given by equations (13) and (78) multiplied by the bidirectional reflectance, that is, the reflectance depending on the direction of the

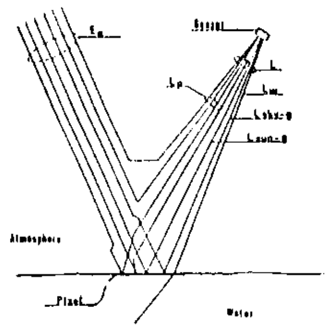

Fig. 18 Component of apparent radiance received by a sensor pointed over the sea. (after Guzzi et al., 1987)

irradiating flux and the direction along which the reflected flux is detected.

Following fig. 19 we can see the bidirectional reflectance depends on i) the angle θ of incidence of the flux at the surface, ii) the azimuthal angle ϕ of the plane of incidence with respect to a direction across the surface, iii) the angle θ to the surface normal from which the flux is detected, iv) the azimuthal angle ϕ of the plane of reflection, v) the solid angle $d\Omega$ subtended by the source at a point on the surface and the solid angle subtended by the entrance pupil of the sensor at the surface.

$$r = r(\lambda, \Delta\lambda; \theta, \theta'; \phi, \phi'; d\Omega, d\Omega'; P, \Delta x, \Delta y, t) \qquad (120)$$

t represents the time dependence that relates seasonal changes to the reflectance of the surface and $\Delta x, \Delta y$ on the dimension of the surface of interest.

Bidirectional reflectance must not be confused with reflectance, since the first has dimension (str^{-1}) while the second is dimensionless. The high dependence of the radiance measured on the geometry of the scene implies the introduction of detection geometry and adjacency effects.

4.1.1 Detection geometry

The geometrical configuration of the sun target sensor drawn in fig. 20 gives us an idea of an interaction between flight direction and sun reflection.

The angular configuration for evaluating the backscattering angle ψ and forward scattering angle ψ_+ are shown in fig. 21 and 22. From this geometry we obtain:

$$\psi_- = \cos^{-1}(-\cos\theta_0 \cos\theta - \sin\theta_0 \sin\theta \cos(\phi - \phi_0)) \qquad (121)$$

and

$$\psi_+ = \cos^{-1}(\cos\theta_0 \cos\theta + \sin\theta_0 \sin\theta \cos(\phi - \phi_0))$$

4.1.2 Adjacency effect

Atmospheric scattering and absorption tend to reduce appreciably the spatial resolution of satellite images of the Earth's surface. In fact the apparent

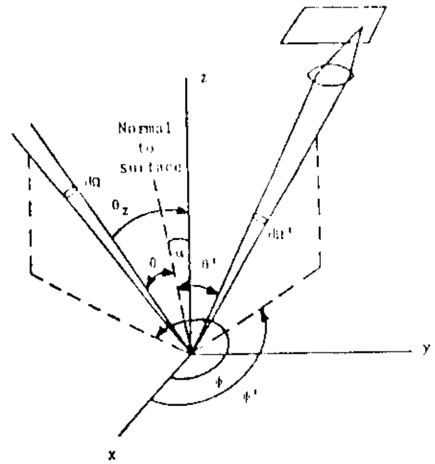

Fig. 10 Geometrical quantities referred to in the bidirectional reflectance distribution function (after Guzzi et al., 1987)

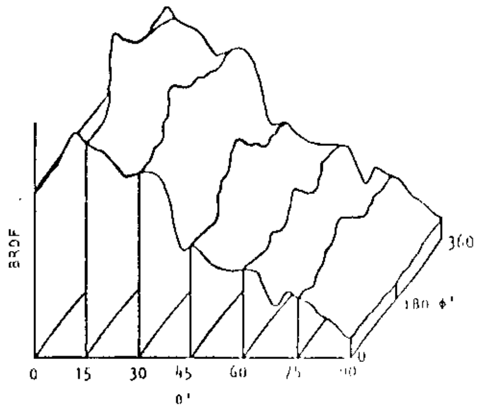

Graphical presentation of BRDF for a particular incident beam angle θ and azimuthal angle $\phi = 360°$.

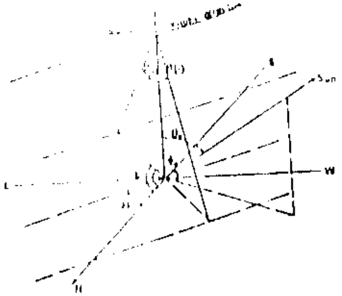

Fig. 20 Geometrical configuration of the sun target sensor (after Guzzi et al., 1987)

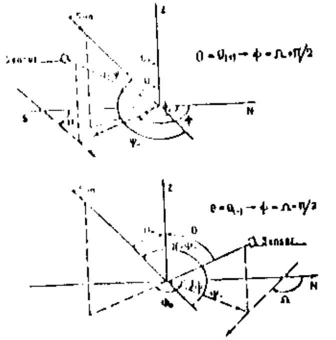

Fig. 21 Angular configuration for evaluation of the backscattering angle ψ_- (after Guzzi et al., 1987)

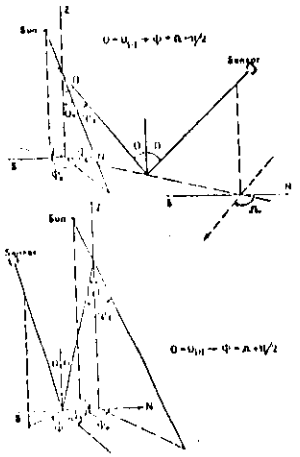

Fig. 22 Angular configuration for evaluation of the forward scattering angle ψ_+ (after Guzzi et al., 1987)

field of view is increased since photons reflected by the surface out of the field of view of the sensor are scattered by the atmosphere into the field of view. This effect is called adjacency effect. The main studies of the effect of atmospheric scattering and absorption on remote sensing imagery are based on the assumption that the surface is uniform. So the combined effect of atmospheric scattering and surface non uniformity greatly affects the accuracy of classification of fields on the Earth's surface that cannot be corrected assuming a uniform surface. The net effect is to transfer light from bright to dark regions.

The transfer function due to atmospheric or sensor effect is drawn in fig. 23. The atmospheric effect is given by the scattering of photons reflected by the surrounding area into the field of view of the sensor; while the sensor effect is due to the finite sensor's footprint that detects the background and the field under test, simultaneously.

The net result is that the atmospheric effect is combined with the sensor characteristics. In such a case the appropriate function describing that result is the total Modulation Transfer Function MTF that is the product of Atmospheric MTF ad sensor MTF. Here we describe the atmospheric MTF.

On the basis of fig. 23 we see the radiance of the light reflected by the earth and the atmosphere is the sum of the following three components: i) path radiance ii) radiance reflected by the surface and directly transmitted through the atmosphere and iii) radiance of light reflected by the surface and then scattered by the atmosphere towards the sensor. While the first component, the path radiance, does not affect the surface reflectance and the second component depends on the reflectance of the viewed field, the third component depends on the reflectance of a nearby field.

In general the magnitude of the three components decreases with the wavelengths, since the optical thickness decreases with wavelength as is shown in fig. 24 and fig. 25 both for dark and bright surfaces. However the atmospheric effect tends to brighten the dark part in the visible and to darken it in the IR.

The brightening is due to dominance of the atmospheric scattering and the darkening is due to dominance of the gaseous and aerosol absorption. Therefore, the atmospheric effect above dark surfaces is very sensitive to the aerosol optical thickness and aerosol scattering phase function, while

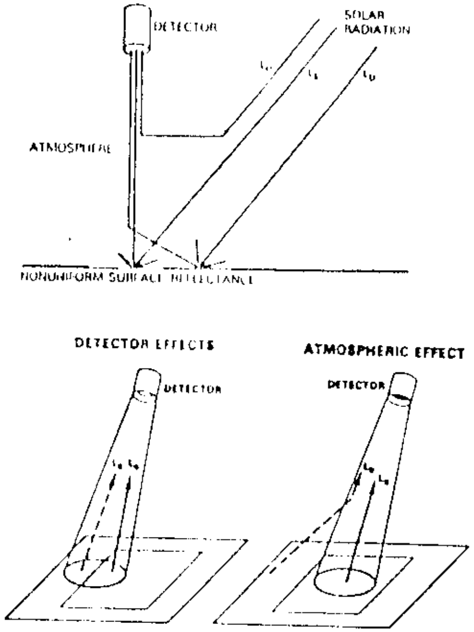

Fig. 23 Schematic diagram of the contribution to the upward radiance (a) and adjacency effect (b)

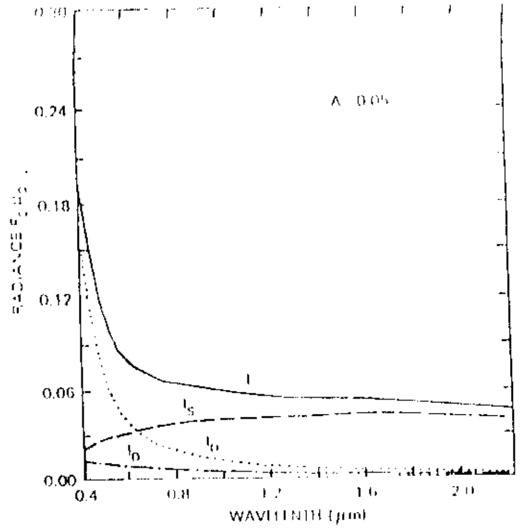

Fig. 24 The upward radiance I and its components I_0, I_s, I_d plotted versus wavelengths for dark reflectivity surface $A = 0.05$. The radiance is normalized to reflectance units and is for nadir observation. The zenith solar angle is 30°. The optical thickness is 0.36 at 0.4μm and 0.07 at 2μm. (after Kaufman, 1984)

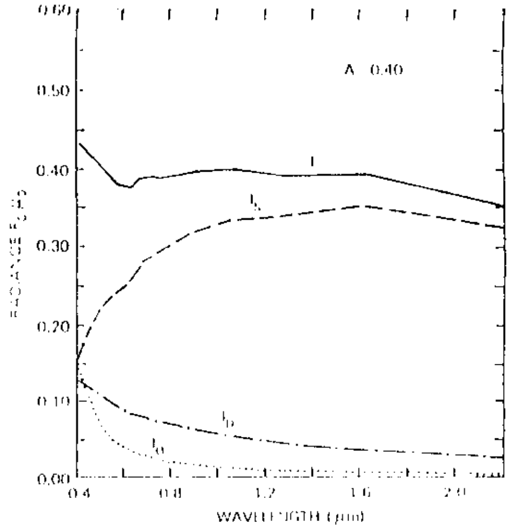

Fig. 25 The same as Fig. 24 but with bright reflectivity surface $A = 0.40$ (after Kaufman, 1984)

the effect above bright surfaces is sensitive mainly to aerosol and gaseous absorption as is shown in fig. 26. It appears that a change in the surface single scattering albedo is more critical than a change in optical thickness over bright surfaces.

The effect of optical thickness is more important over the dark surface. The atmospheric effect depends also on the zenith angle of observation as shown in fig. 27 and fig. 28 on a change of atmospheric haziness as is shown in fig. 29. In the first case of fig. 29 the path radiance decreases as the reflectance of the background decreases, while the bright background causes a strong increase in the total radiance. In the second case the increase is very small. In the third case the dark background causes a decreasing in the radiance. In conclusion the radiance for the same atmosphere may increase or decrease depending on the relative brightness of the field and its background.

The effect of the background brightness on the radiance, the so called adjacency effect is presented in fig. 30 a, b where the results shown are calculated by rescaling the Monte Carlo radiances (Pearce, 1977) to lower contrast in the surface reflectance (Kaufman, 1984). In case *a.* as aerosol optical thickness increases the upward radiance increases for large fields and decreases for small fields. The increasing and decreasing correspond respectively to fig. 29 b and 29 c. In case *b.* of a black field surrounded by a field of 0.2 reflectivity (i. e. lake surrounded by vegetation), the adjacency effect acts on the observed radiance much more than the atmospheric effect producing a misclassification of small water bodies detected from remotely sensed imagery.

The atmospheric MTF describes the attenuation of the direct reflected radiance and the effect of the diffuse reflected radiance that tends to decrease the radiance above bright targets.

Therefore, the atmospheric MTF gives the relative depression of spatial frequencies ω of an object by a hazy atmosphere and is defined by the ratio:

$$M(\omega) = F[L^N(x,y)]/F[r(x,y)] \qquad (122)$$

where F represents the Fourier transform, $r(x,y)$ the surface reflectance and $L^N(x,y)$ the upward radiance out of the atmosphere normalized to reflectance units.

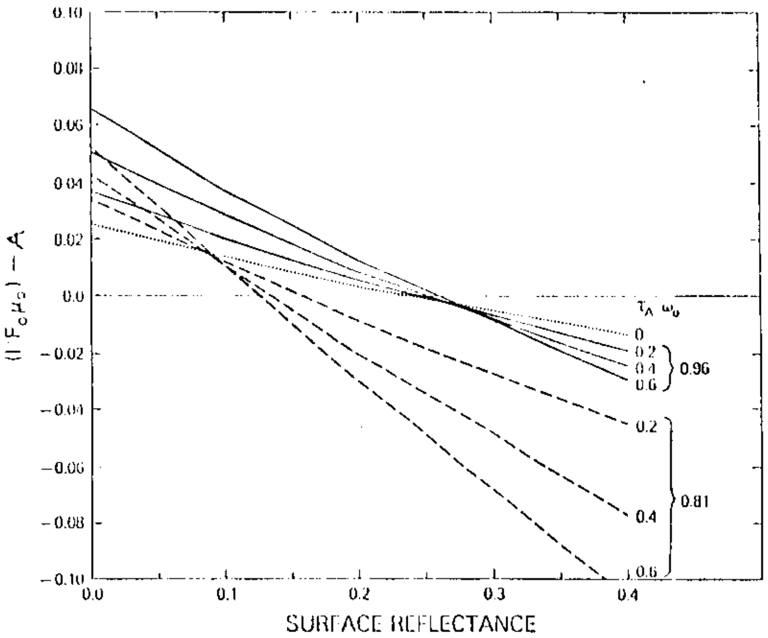

Fig. 20 The difference between the normalized upward radiance at nadir and the surface reflectance. Thin solid line: zero difference (no absorption). Dotted line: clear atmosphere. Thick solid line: varying aerosol optical thickness (τ_a). Dashed line: high absorption ($\omega_0 = 0.81$). Solar zenith angle is 40° and $\lambda = 0.6 \mu m$ (after Kaufman, 1984)

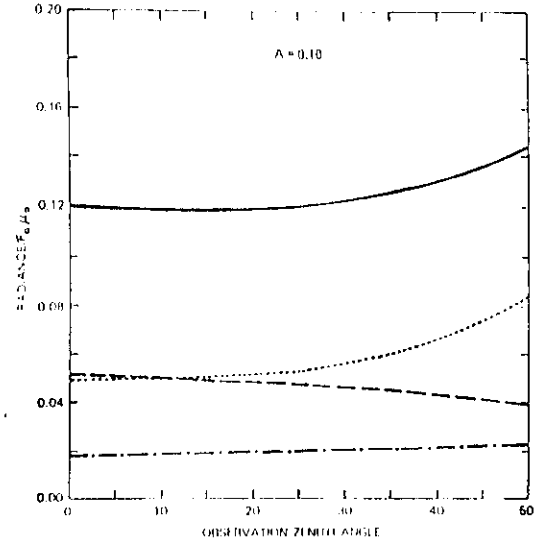

Fig. **27** The same as Fig. 25 as a function of observation zenith angle for dark surface $A = 0.10$. The solar zenith angle is 30°. $\tau_a = 0.5$ at $\lambda = 0.6\mu m$ (after Kaufman, 1984)

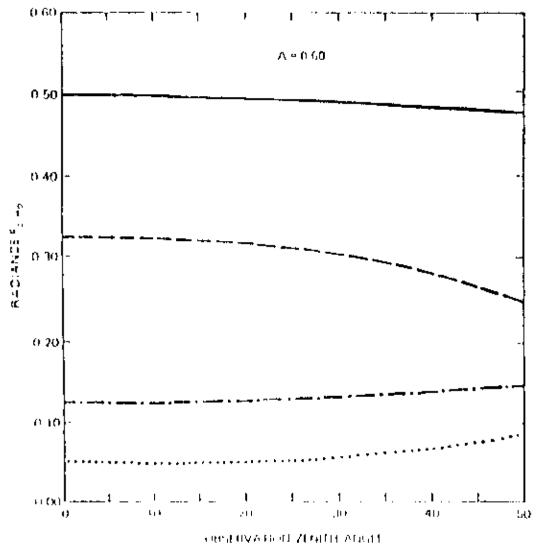

Fig. **28** The same as Fig. 27 for bright surface $A = 0.60$ (after Kaufman, 1984)

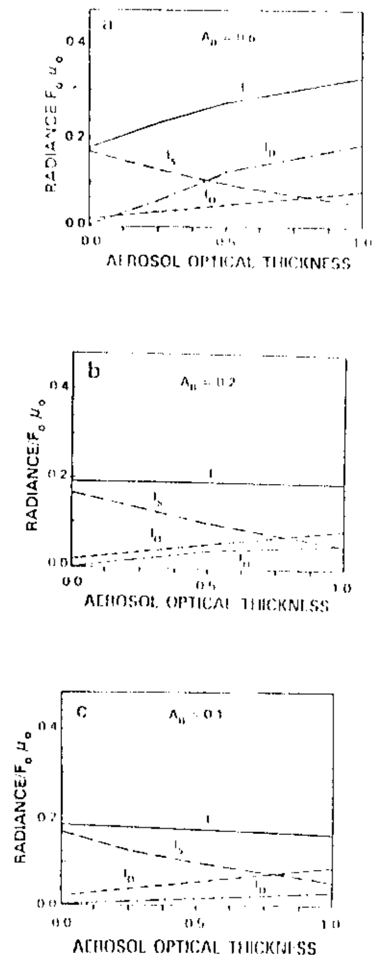

Fig. 29 Atmospheric effect on the upward radiance. The upward radiance at zenith normalized to reflectance units is plotted as a function of the aerosol optical thickness. The radiance is for an infinitesimal small field of reflectance $A_s = 0.2$. The background reflectance A_B is indicated in each figure. The calculation were performed for $\theta_0 = 30°$ at $\lambda = 0.55\mu m$; aerosol refractive index $n_a = 1.43 - 0.0035i$ (after Kaufman, 1984)

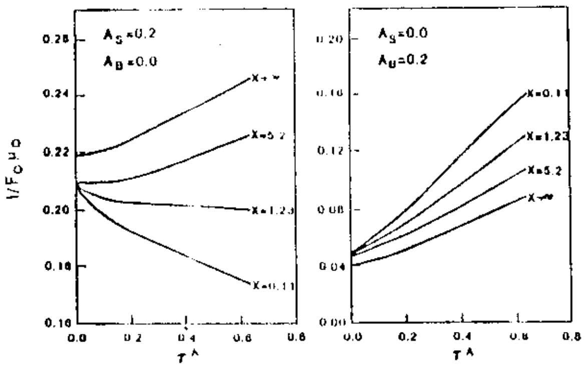

Fig. 30 Reflectivity of the earth - atmosphere system in the direction toward the center of a square target located at the nadir. The length of a side is given by X in Km. The reflectivity of the target and of the background are A_s and A_B respectively. The solar zenithangle is $40°; \lambda = 0.55\mu m; n_a = 1.5$. (after Kaufman, 1984)

The normalized MTF as a function of the spatial frequency has been calculated by Pearce (1977) by Monte Carlo calculations and by Mekler and Kaufman (1980) through semianalytical approximations. However simulation analysis Kaufman (1984) gives the following empirical approximated formula:

$$M^N(\omega) = 1 - 0.5\tau_R[1 - \exp\{-2.5\omega H_R\}] - \\ -0.7\lambda^{-0.2}\tau_a[1 - \exp\{+1.3\omega H_a\}] \qquad (123)$$

depending on spatial frequency ω for a given molecular optical thickness τ_R, aerosol optical thickness τ_a, molecular and aerosol scale heights H_R, H_a and wavelenght λ and valid in the range $470 - 1650 nm$. The comparison between Monte Carlo simulation curve and the empirical gives an error of less than 10%.

The absolute atmospheric MTF can be obtained by multiplying the normalized MTF by MTF value at $\omega = 0$. The MTF (0) can be calculated by the definition of the MTF itself. For definition (Pearce, 1977) the MTF is the contrast between max and min above a sinusoidal surface reflectance

$$M(\omega) = \frac{L_{max}(\omega) - L_{min}(\omega)}{2\Delta r F_0 \mu_0} \qquad (124)$$

where $L_{max}(\omega)$ and $L_{min}(\omega)$ are the radiances above the maximum and the minimum respectively with the difference in surface reflectance of $2\Delta r$. π_0 is the incident solar flux and μ_0 the cosine of solar zenith angle. For $\omega \rightarrow 0$ the distance between *min* and *max* are very large and the radiances can be written as:

$$L(0)_{max} = L_0 + xF_D[exp(-\tau_0) + t](r + \Delta r)/\pi F_0 \\ L(0)_{min} = L_0 + xF_D[exp(-\tau_0) + t](r - \Delta r)/\pi F_0 \qquad (125)$$

where $L_0 = L(r = 0)$ is the radiance for zero surface reflectance; F_D is the downward total flux (average diffuse plus direct); τ_0 is the total atmospheric optical thickness and t the diffuse transmittance through the atmosphere to the zenith. Then:

$$M(0) = F_D[\exp(-\tau) + t]/\pi F_0 \mu_0 \qquad (126)$$

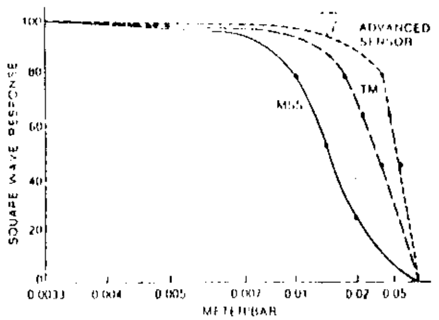

Fig. 31 Square wave response of the Landsat TM and MSS sensors. The advanced sensor curve was obtained from TM curve for twice the resolution ($15m$) (after Kaufman, 1984)

Sensor	MSS		TM		Advanced sensor	
Response	0.35	0.5	0.35	0.5	0.35	0.5
Sensor only	70	90	30	40	15	20
Sensor and atmosphere	170	790	100	830	50	710
Sensor and corrected atmosphere	95	140	50	85	22	45

Table 6: Spatial Resolution (in Meters) of Three Sensors for Two Responses

So equation (123) can be multiplied by the sensor's MTF (see fig. 31 for the MTF of different sensors) to yield the total MTF of the system $M^*(\omega)$.

Then the upward radiance $L(x, y)$ detected by the sensor above a surface with reflectivity $r(x, y)$ can be written:

$$L(x, y) = L_0 + F^{-1}\{M^*(\omega)F[r(x, y)]\} F_0\mu_0 \quad (127)$$

where: $\omega^2 = \omega_x^2 + \omega_y^2$. An example of total MTF $M^*(\omega)$ as a function of spatial frequency (cycles/km) is shown in fig. 32. In this figure the atmospheric MTF was computed for a solar zenith angle of 20 degrees, $\lambda = 0.5\mu m$ and aerosol thickness of 0.5. In this case the spatial resolution given by the field edge length for a given value of MTF, is smaller than the resolution without the atmosphere.

On the basis of the knowledge of atmospheric characteristics it is possible to correct the total $MTF : M^*(\omega)$. The correction is obtained from the uncorrected MTF (short dashed line) by dividing it by its values at $\omega = 0$ i. e. $M(0)$.

In Table 6 the spatial resolution in meters of three sensors for two given MTF are tabulated. It is evident that the apparent resolution depends not

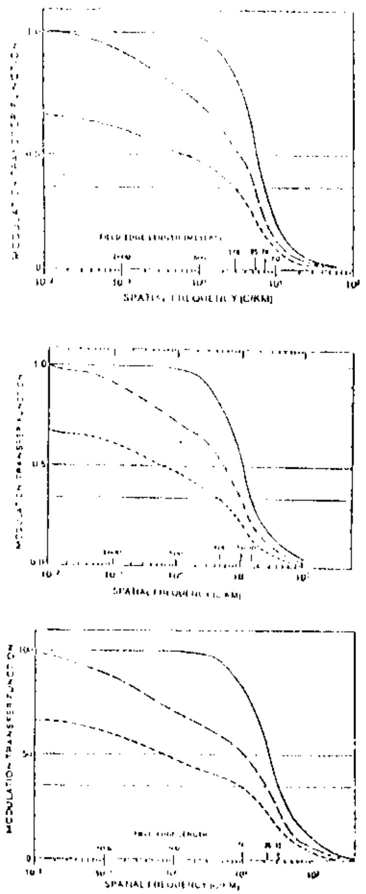

Fig. 32

a. Landsat MSS MTF curve (solid line). Short dashed line: atmospheric effect with $\tau_a = 0.5$ at $\lambda = 0.55\mu m$. Long dashed line: atmospheric effect with correction for a uniform surface. Thin lines are the MTF values at 0.35 and 0.5 (after Kaufman, 1984)

b. Same as a. but for Landsat TM sensor (after Kaufman, 1984)

c. Same as a. but for advanced sensor (after Kaufman, 1984)

only on the spatial resolution of the sensor but also on the entire curve of the sensor's MTF.

4.1.3 Note on the Modulation Transfer Function MTF

The MTF is a quantitative measure of quality image. MTF describes the ability of a system to transfer object contrast to the image as a function of spatial frequency. Consider a sine wave chart in the form of a positive transparency on which transmittance varies one-dimensionally in a precisely sinusoidal fashion. Assume the transparency is viewed against a uniformely illuminated background. The max and min transmittance are T_{max} and T_{min} respectively. A lens system, under test, forms a real image of sine wave chart, and the spatial frequency of the image is ω (cycles mm^{-1}). Corresponding to the transmittance T_{max} and T_{min} are the image irradiances I_{max} and I_{min}. The contrast or modulation of the chart and image are respectively defined by:

$$M_c = \frac{T_{max} - T_{min}}{T_{max} + T_{min}}$$

$$M_i = \frac{I_{max} - I_{min}}{I_{max} + I_{min}}$$

Then the Modulation Transfer Function is:

$$MTF(\omega) = \frac{M_i}{M_c} \quad (128)$$

A plot of MTF against spatial frequency is shown in Fig. 33. Since the spatial frequency of interest is given, for a satellite system, (sensor plus detector) by the Effective Instantaneous Field of View (EIFOV), which corresponds to the 0.5 MTF values, the conversion of spatial frequency to a distance is given by the reciprocal of twice this spatial frequency (see also Fig. 32).

Pearce, 1977, defines the atmospheric MTF as the amplitude attenuation of an input sine wave of the surface reflectance with spatial frequency ω whose spacing between each two maxima of the sine waves is $1/\omega$.

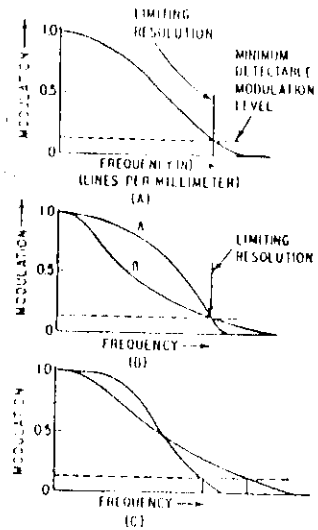

Fig. 33 Image modulation as a function of frequency of the test pattern.

a. The intersection of the modulation function line with a horizontal line gives the smallest amount of modulation which the system can detect.

b. Two modulation plots with the same limiting resolution but quite different performances. The system with greater modulation at lower frequency is superior.

c. Two systems, one exhibit high limiting resolution, the other high contrast at low target frequency. In case of this type, the decision must be based on the relative importance of contrast versus resolution in the function of the system.

4.1.4 Bidirectional reflectance over the sea

An algoritm for the bidirectional reflectance over the sea has been proposed by Cox and Munk. It is given by:

$$r(\xi, \beta, v) = p(\beta, v) \frac{\cos \xi}{4 \cos^3 \beta} \tag{129}$$

where

$$p(\beta, v) = \frac{1}{\pi \sigma^2} \exp\left\{-tan^2 \beta / \sigma^2\right\} \tag{130}$$

is the probability function for the direct sun radiance reflected by the surface as a function of wind speed v and angle β, see fig. 34.

$$\sigma^2 = 0.003 + 0.00512 v (m/sec)$$

with

$$\begin{aligned} \beta &= \cos^{-1}\left(\frac{\cos\theta + \cos\theta_0}{2\cos w}\right) \\ \xi &= \cos^{-1}\left[\frac{1}{2}(1 + \cos\psi)\right]^{0.5} \\ \psi &= \cos^{-1}\left[\cos\theta_0 \cos\theta + \sin\theta_0 \sin\theta \cos(\phi - \phi_0)\right] \end{aligned} \tag{131}$$

4.1.5 Bidirectional reflectance from ground

From the definition of bidirectional reflectance in eq. (120) it is evident that it relates the directional radiance of the surface to the directional irradiance and directional source radiance. With respect to the algoritm proposed for the sea the bidirectional reflectance from the ground is influenced by the vegetative canopy. The spectral reflectance of vegetative canopy is, however, influenced by reflectance of the soil present and in particular for crops with incomplete covers. Fig. 34 shows the comparison between green wheat leaf and dry ($Q = 1$) and wet ($Q = 6$) sandy loam soil.

Directional reflectance $r(\theta_0, \theta_s, \psi, s)$ is defined by:

$$r(\theta, \theta_0, \phi, s) = \frac{\pi L(\theta_0, \theta_S, \phi, s)}{E_0(\theta, s) + E_s(\theta, s)} \tag{132}$$

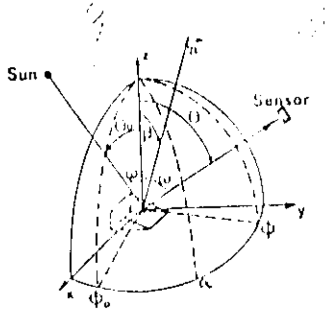

Fig. 34 Geometrical configuration of sun glitter reflection over the sea. (after Guzzi et al., 1987)

where θ is the zenith observation angle $\theta_0$zenith solar angle, s is the leaf inclination interval, $E_0(0,s)$ is the incident solar direct flux over the leaf inclined of s and $E_-(0,s)$ is the sky irradiance. The radiance structure depends on the geometry of the canopy layers.

A complete overview of the theories and applications can be found in Bunnik (1978).

In fig. 35, 36, 37 bidirectional reflectance and albedo of several surfaces are reported.

4.2 Application of the passive Remote Sensing techniques to selected case studies

4.2.1 Measurements performed in the visible and near infrared of water leaving radiance and aerosol load

In order to perform measurements over the sea we apply equation (119). It requires also the introduction of the water leaving radiance $L_w(\lambda)$ added to the other factors. That is, we take into account the radiance emerging from the sea bulk and reaching the sensor. The use of new relation 119 does not account for aerosol variability in time and space. However, the experimental data can be corrected by evaluating the aerosol load from the image corresponding to wavelength in the near infrared region where the sea water reflectance is almost equal to zero (see fig. 37). Then the procedure to be adopted assumes the radiance emerging from the water is negligible at wavelengths $\lambda \geq \lambda_{nir}$. Total optical thickness of the aerosol can be obtained by imposing that the aerosol optical thickness is smaller than a maximum value $\tau_A(\lambda) = \Gamma$.

On this basis we can adopt the following procedure:

1.

$$\tau_A(\lambda) = \frac{1}{2}\Gamma$$

and

$$\Delta\tau_A(\lambda) = \frac{1}{2}\Gamma \qquad (133)$$

and evaluate

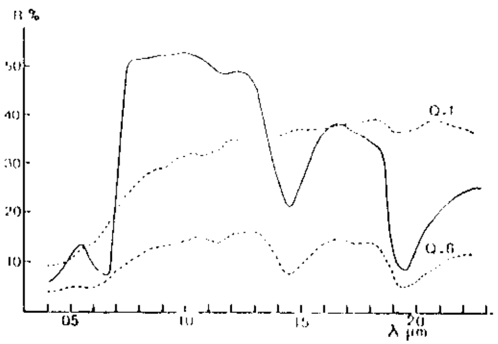

Fig. 35 Spectral reflectance of a green wheat leap compared with reflectance of a dry ($q = 1$) and a moist ($q = 6$) sandy loam soil (after Bunnik, 1978)

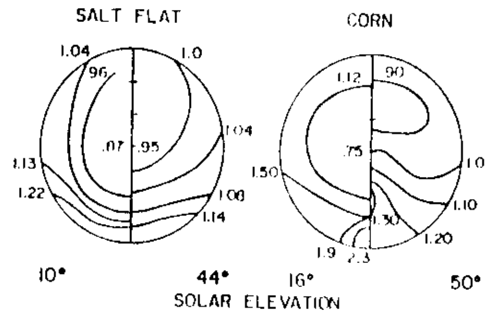

Fig. 36 Bidirectional reflectance function of Bonneville, Utah, Salt Flat and corn field each for low and high solar elevation. Albedo for a horizontal receiver in the spectral range 0.3 – $3\mu m$ (after Eaton and Dirmhin, 1979)

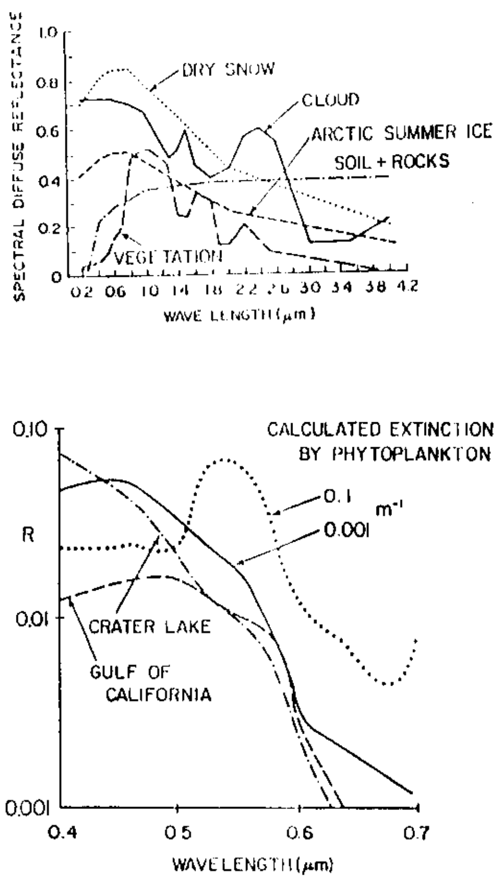

Fig. 37

a. Typical spectral diffuse reflectance of different surfaces

b. Nadir reflectance in the spectral range $0.4 - 0.7 \mu m$ (after Suits, 1978)

2.

$$L_{sung}(\lambda), L_{skyg}(\lambda) and L_p(\lambda)$$

through the algoritms of chapter 3.

3. The interactive process is stopped if the relation $|s| \leq r$ is satisfied (r is evaluated taking into account the digitation error of data) when:

$$s = L(\lambda) - L_{sung}(\lambda) - L_{skyg}(\lambda) - L_p(\lambda) \qquad (134)$$

4. Otherwise we assume $\Delta\tau_A = \Delta\tau_A/2$ and we impose

$$\tau_A(\lambda) = \tau_A(\lambda) - \Delta\tau_a \qquad for \qquad s < 0$$

$$\tau_A(\lambda) = \tau_A(\lambda) - \Delta\tau_a \qquad for \qquad s > 0$$

and resuming from step 2.

At wavelengths at which the water leaving radiance is very low or negligible it is possible to make a comparison between retrieved optical thickness and that measured from a ground instrument. In fig. 38, 39 are presented data obtained by Zibordi and Maracci (1988) using the model herein proposed and comparing the results with ground measurements performed by a photometer.

Once the optical thickness has been determined it is possible to apply the results to equation (119) and calculate the atmospheric component.

The difference between measured radiance and computed atmospheric radiance gives the water leaving radiance.

Fig. 40, 41, 42, 43, 44, 45, show the technique adopted and the magnitude of different components of the model. Finally computed spectral water leaving radiance is presented in fig. 46, 47, 48.

4.2.2 Vegetation index

To estimate the photosyntetic capacity of the land, polar orbiting satellite data from AVHRR sensor channels has been extensively used. Channels

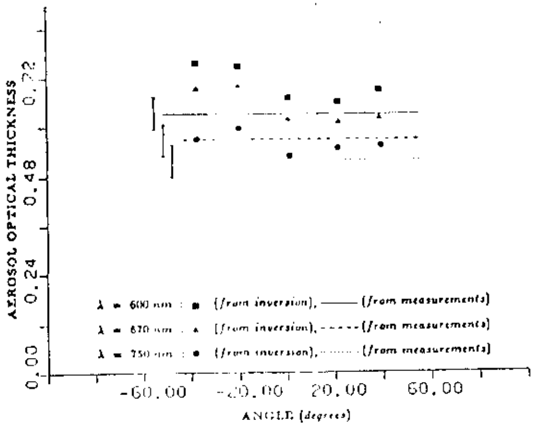

Fig. [illegible] Comparison between aerosol optical thickness obtained from measurements of atmospheric transmittance and inversion of remotely sensed data (after Zibordi and Maracci, 1988)

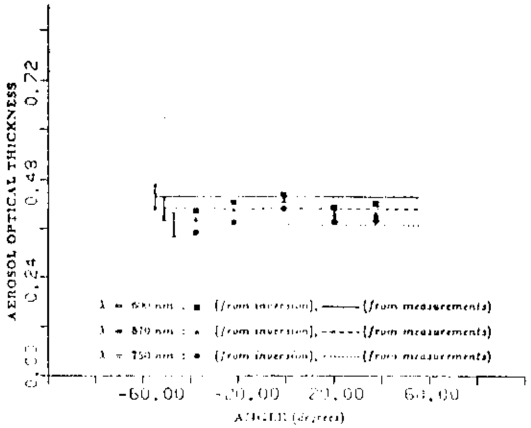

Fig. 39 Same as Fig. 38 but for a different day (after Zibordi and Maracci, 1988)

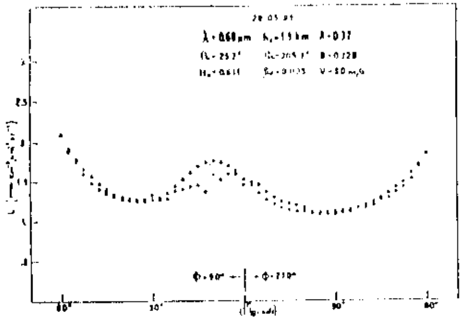

Fig. 40 Comparison between values of apparent radiance calculated (triangles) and measured (dots) at $\lambda = 0.68\mu m$ and altitude $= 1.5 km$ (after Guzzi et al., 1987)

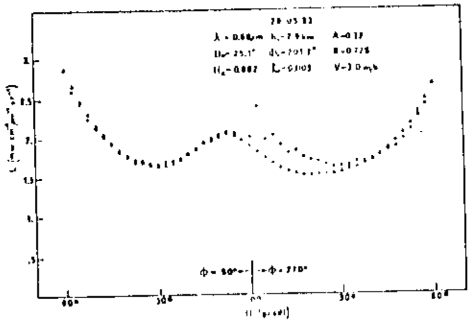

Fig. 41 Same as Fig. 40 but at altitude $= 2.9 km$ (after Guzzi et al., 1987)

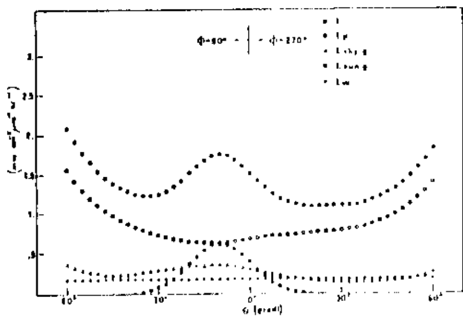

Fig. 42 Values of the different contributions to the theoretical data of the apparent radiance proposed in Fig. 40 (after Guzzi et al., 1987)

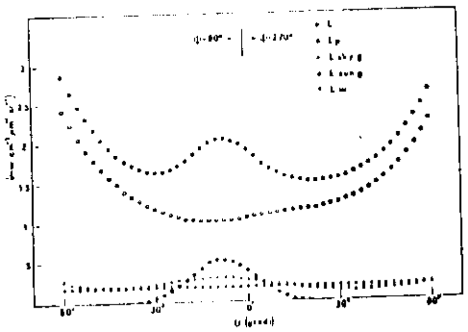

Fig. 43 Same as Fig. 42 but for Fig. 41 (after Guzzi et al., 1987)

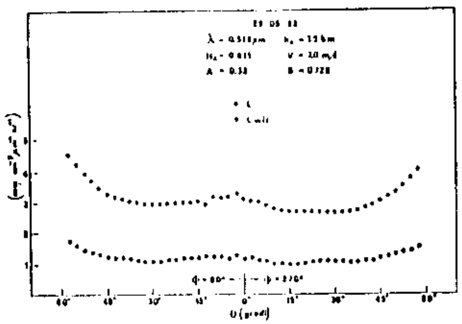

Fig. 44 Values of water leaving radiance L_{wlr} with respect to the apparent radiance L at $\lambda = 0.519\mu m$ and altitude $= 1.5km$ (after Guzzi et al., 1987)

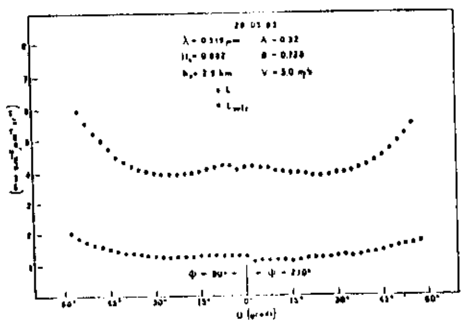

Fig. 45 Same as Fig. 44 but with altitude $= 2.9km$ (after Guzzi et al., 1987)

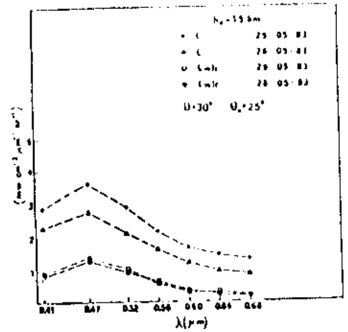

Fig. 46 Comparison between values of data obtained at altitude $1.5km$ and different turbidities (after Guzzi et al., 1987)

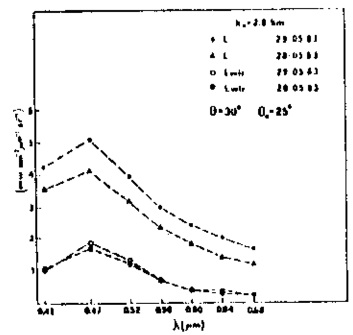

Fig. 47 Same as Fig. 46 but with altitude $= 2.9km$ (after Guzzi et al., 1987)

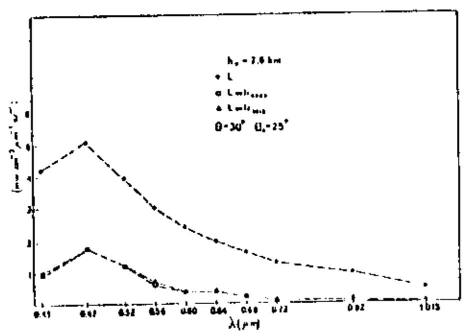

Fig. 48 Comparison between spectral water leaving radiance (after Guzzi et al., 1987)

1(0.55 − 0.68μm) and 2(0.72 − 1.1μm) were used to produce the Normalized Difference Vegetation Index (NDVI) defined as:

$$NDVI = \frac{D_2 - D_1}{D_2 + D_1} \tag{135}$$

where D_1 and D_2 are digital numbers respectively in channels 1 and 2.

Satellite-sensor radiance $L(\lambda_i)$ for the Julian day J can be written as:

$$L(\lambda_i) = (a_i D_i + b_i) \cdot \left((1 + e\cos(\frac{2\pi(J-3)}{365}))\right)^2 \tag{136}$$

where:

$$a_i = G_i E(\lambda_i)/100\pi$$
$$b_i = I_i E(\lambda_i)/100\pi$$
$$E(\lambda_i) = \int_0^\infty \overline{E}_0(\lambda_i')\phi(\lambda_i')d\lambda_i' \tag{137}$$

G_i and I_i are percentage albedo for count and percentage intercept for channel i; $\overline{E}_0(\lambda_i)$ is the solar irradiance at the top of the atmosphere per unit area for mean Sun-Earth distance; $\phi(\lambda_i)$ is the spectral response function of the sensor, e is Earth eccentricity. Thus, for a given day J, a_i and b_i are known. Solving equation (136) for D_i gives:

$$D_i = \alpha_i L(\lambda_i) + \beta_i \tag{138}$$

where:

$$\alpha_i = \frac{1}{a_i}, \qquad \beta_i = -\frac{b_i}{a_i} = -\frac{I_i}{G_i}$$

and substituting in equation (135) we obtain:

$$NDVI = \frac{\alpha_2 L(\lambda_2) - \alpha_2 L(\lambda_1) + \beta_2 - \beta_1}{\alpha_2 L(\lambda_2) + \alpha_1 L(\lambda_1) + \beta_2 + \beta_1} \tag{139}$$

Since the radiance measured by satellite sensor can be also written as:

$$L(\lambda_i) = L_p(\lambda_i) + L_s(\lambda_i)t(\lambda_i) \tag{140}$$

where $L_p(\lambda)$ is the path radiance; $L_s(\lambda_i)$ the surface leaving radiance and $T(\lambda_i)$ is the pixel to sensor diffuse transmittance.

The spectral reflectance is defined as:

$$r(\lambda_i) = \frac{\pi L_s(\lambda_i)}{E_g(\lambda_i)} \tag{141}$$

substituting L_s from equation (141) to equation (140) and resulting in equation (139) we obtain:

$$NDVI = \frac{X_s^- + X_p^- + \pi(\beta_2 - \beta_1)}{X_s^+ + X_p^+ + \pi(\beta_2 + \beta_1)} \tag{142}$$

where s and p stand for surface reflectance and atmospheric path radiance information and:

$$X_s^{\pm} = \alpha_2 r(\lambda_2)E_g(\lambda_2)t(\lambda_2) \pm \alpha_1 r(\lambda_1)E_g(\lambda_1)t(\lambda_1)$$

$$X_p^{+} = \pi[\alpha_2 L_p(\lambda_2) + \alpha_1 L_p(\lambda_1)]$$

The global irradiance $E_g(\lambda)$ as a function of solar zenith angle, θ_0, and direct irradiance $E_d(\lambda)$ can be estimated by the following empirical expression proposed by Singh et al. (1985) and valid for $\theta_0 < 70°$:

$$E_g(\lambda) = E_d(\lambda)[1 + R(\lambda, \theta_0)] \tag{143}$$

where:

$$ln[R(\lambda, \theta_0)] = -4.872 + 0.35\theta_0 + \frac{1.442}{\lambda} + 0.172\frac{\theta_0}{\lambda}$$

with θ_0 in radians and λ in μm. Simulated NDVI for various surface cover types presented in Table 7 as a function of θ_0 is shown in fig. 49.

4.2.3 Ground temperature measured by airborne platform

The actual temperature of the surface can be obtained by the apparent spectral radiance measured by the onboard airborne platform sensors at altitude z.

	Reflectance $\rho(\lambda)$		Surface NDVI
Class †	Channel 1	Channel 2	NDVI= $[\rho(\lambda_2) - \rho(\lambda_1)]/[\rho(\lambda_1) + \rho(\lambda_2)]$
I	0.03	0.04	0.86
II	0.05	0.25	0.67
III	0.10	0.20	0.33
IV	0.20	0.25	0.11

Table 7: Input surface reflectances for the simulation algorithm for various surface-cover types (source Holben, reported by Singh) † Class I, high green-leaf vegetation density; class II, moderate green-leaf vegetation density; class III, low green-leaf vegetation density; class IV, bare soil.

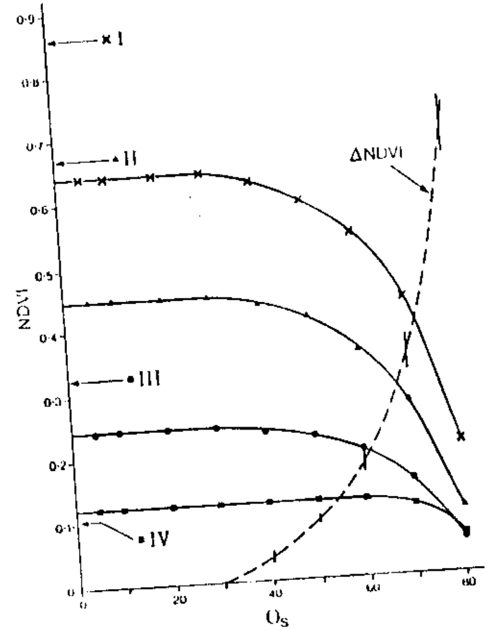

Fig. 49 The simulated NDVI for NOAA7 and AVHRR data from nadir view as a function of solar zenith angle θ_0. The four classes of cloud cover types are listed in Table 7. Arrows indicate the surface value of NDVI. (after Singh, 1988)

C References

Bignell J. K., 1970, *The water vapour infra-red continuum*, Q. J. R. Met. Soc., vol. 96, pp. 390-403

Bunnik N. J. J., 1978, *The multispectral reflectance of short wave radiation by agricultural crops in relation with their morphological and optical properties*, H. Veenman and Zonen B. V. Wageningen

Burch D. E. , 1970,*Investigation of the absorption of infrared radiation by atmospheric gases*, semi annual Rep. publ., U-4784, Aeronutronic Div. Philco-Ford Co., Newport Beach, Calif.,

Eaton F. D. and I. Dirmhirn, 1979, *Reflected irradiance indicatrices of natural surfaces and their effect on albedo*, Applied Optics, vol. 18

Elterman L., 1970 *Vertical-attenuation model with eight surface meteorological Ranges 2 to 13 km*, 1970 AFCRL Report No. 70-0200, Air Force Cambridge Research, Lab. Redford, Mass.

Fröhlich C., 1988, *Extraterrestrial Solar Radiation*, 1988, Physical climatology for solar and wind energy, Editors R. Guzzi and C. Justus World Scientific Co. Singapore, pp. 38-55

Gordon H. R., D. K. Clark, J. W. Brown, O. B. Brown, R. H. Evans and W. W. Broenkow, 1983, *Phytoplankton pigment concentrations in the middle Atlantic Eight: comparison of ship determination and CZCS estimates*, Applied Optics, vol. 22, pp.20-36

Goody R. M., 1964, *Atmospheric Radiation I Theoretical basis*, Oxford University Press

Grassl H., 1974, *Influence of different absorbers in the window region on radiative cooling (and on surface determination)* contr. Atmos. Phys., vol.47, pp.1-13

Guzzi R., 1988, *Atmospheric structure and an introduction to the electromagnetic processes in the atmosphere*, Physical Climatology for Solar and Wind Energy, Editors R. Guzzi C. G. Justus, World Scientific Co. Singapore, pp. 3-37

Guzzi R. and R. Rizzi, 1980, *The effect of radiative exchange on the growth by condensation of a population of droplets*, Contribution to Atmospheric Physics, vol. 53

Kaufman Y. J., 1984, *Atmosferic effect on remote sensing of surface reflectance*, SPIE, vol. 475, pp 20-33

Kaufman Y. J., 1984, *Atmospheric effect on spatial resolution of surface imagery: errata*, Applied Optics, vol. 23, pp. 4164-4172

Kaufman Y. J. and R. S. Fraser, 1984,*Atmospheric effect on classification of finite fields*, Remote Sensing of Environ vol. 15, pp. 95-118

Kneizys F. X., E. P. Shettle, W. O. Gallery, J. H. Chetwynd, L. W. Abreu, J. E. A. Selby, S. A. Clough, R. W. Fenn, 1983, *Atmospheric Transmittance/Radiance: Computer code Lowtran 6* , AFGL-TR-83-0187 Env. Res. paper No. 846 Air Force Geoph. Lab., Hanscom AFB, Mass. 01731

Lacis A. A. and J. Hansen, 1974, *A Parameterization for the Absorption of Solar Radiation in the Earth's Atmosphere*, J. Atmos Sci, vol. 3, pp. 118

Leckner B., 1978, *The spectral distribution of solar radiation on the earth's surface*, Solar Energy, vol. 20, pp. 1443-150

Lenoble J. editor, 1985, *Radiative transfer in scattering and absorbing atmosphere: standard computational procedures*, A. Deepak Publishing, Virginia

Liou Kuo-Nan, 1985, *An Introduction to Atmospheric Radiation*, Academic Press, pp. 184-192

Meckler Y., Y. J. Kaufman, 1980, *The effect of earth's atmosphere on contrast reduction for a nonuniform surface albedo* *and two-halves field*, Journal of Geophysical Research, vol. 85 No. C7, pp. 4067-4083

McMillin L. M., 1975, *Estimation of sea surface temperature from two infrared window measurements with different absorption*, J. Geophys. Res., vol. 88, pp. 5113-5117

Paltridge G. W. and C. M. R. Platt, 1976, *Radiative Processes in Meteorology and Climatology*, Elsevier Sci Pub. Co., Amsterdam

Pearce W. A., 1977, *A study of the effects of the atmosphere on Thematic Mapper observation*, Rep. 004-77 EG G, Washington Anal. Serv. Center, Riverdale, Maryland, p.136

Reitan C. H., *Surface Dew Point and Water Vapor Aloft*, 1963, J. App. Meteor., vol. 2, pp. 776

Rodgers C. D., and C. D. Walshaw, 1966, *The computation of infra-red cooling rate in planetary atmospheres*, Q. J. R. Meteorol. Soc., 92, pp 67-92

Schuster A., *Radiation through foggy Atmospheres*, Astrophys. J., 1905, 21 p 1

Singh S. M., 1985, *Remarks on the use of Stefan Bolzman type relation for estimating surface temperature*, Int. J. Remote Sensing, 1985, vol. 6, pp. 741-747

Singh S. M., A. P. Cracknell and D. Spitzer, 1985, *Evaluation of sensitivity decay of Coastal Zone Color Scanner (CZCS) detectors by comparison with in situ near surface radiance measurements*, Int. J. Remote Sensing 6, pp. 749-758

Singh S. M., 1988, *Simulation of solar zenith angle effect on global vegetation index (GVI) data*, Int. J. Remote Sensing 9, pp. 237-243

Sobolev V. V., 1963, *A Treatise on Radiative Transfer*, Van Nostrand, Princeton N. J.

Suits G. M., 1978, *The natural sources*, The infrared Handbook edited by W. L. Wolfe and G. L. Zissis, Office of Naval Research Washington D. C.

Tomasi C., R. Guzzi and O. Vittori, 1974, *A search for e-effect in the water vapor continuum*, J. Atmosph. sci, vol. 31, pp. 255-260

Turner R., 1973, *Radiative Transfer in real Atmospheres*, NASA CR-140199 ERIM 19010024 T

Van Stokkom A. T. C. and R. Guzzi, 1984, *Atmospheric spectral attenuation of airborne remote sensing data: Comparison between experimental and theoretical approach*, Int. J. Remote Sensing, vol. 5, pp. 925

Zibordi G., G. C. Maracci, 1988, *Determination of atmospheric turbidity from remotely sensed data*, Int. J. Remote Sensing, vol. 19, pp. 1881-1894